USGS Award No. 06HQGR0057

A PROBABILISTIC APPROACH FOR EVALUATING NEWMARK SLOPE DEFORMATIONS

FINAL TECHNICAL REPORT

Ellen M. Rathje, Ph.D., P.E.
University of Texas at Austin
ECJ 9.227, C1792
Austin, TX 78712
Tel: 512-471-4929
Fax: 512-471-6548
e.rathje@mail.utexas.edu
http://www.ce.utexas.edu/dept/area/geotech/GeotechnicalEngr.htm

NEHRP Element: II
Key Words: Earthquake-Induced Landslides, Sliding Deformation, Seismic Hazard

Research supported by the U.S. Geological Survey (USGS), Department of the Interior, under USGS award number (06HQGR0057). The views and conclusions contained in this document are those of the authors and should not be interpreted as necessarily representing the official policies, either expressed or implied, of the U.S. Government

ABSTRACT

The objective of this research is to develop scalar and vector hazard methodologies to predict the earthquake-induced sliding displacement of slopes. This work encompasses generation of empirical models that predict sliding displacement as a function of single ground motion parameters and vectors of ground motion parameters. These models also quantify the uncertainty (standard deviation) in the sliding displacement prediction. The most appropriate scalar parameters and vectors of parameters are identified, and their ability to minimize the standard deviation in the prediction is evaluated. The scalar and vector probabilistic frameworks are outlined and used, along with the developed empirical displacement models, in an example calculation for a hypothetical slope. Comparisons between the different probabilistic approaches, as well with a deterministic approach, are provided.

NON-TECHNICAL SUMMARY

Earthquake-induced sliding displacement is the parameter most often used to assess the seismic stability of slopes. The expected displacement can be predicted as a function of the characteristics of the slope and the parameters representing the ground motion (e.g., peak ground acceleration). However, there is significant uncertainty in both the prediction of the ground motion parameters and slope displacement. The proposed probabilistic methodology allows for a rational incorporation of these uncertainties in the prediction of the earthquake-induced sliding displacements of slopes.

INTRODUCTION

The seismic performance of slopes and earth structures is often assessed by calculating the permanent, downslope sliding displacement expected during earthquake shaking. Newmark (1965) first proposed a rigid sliding block procedure, and this procedure is still the basis of many analytical techniques used to evaluate the stability of slopes during earthquakes. Newmark (1965) realized that accelerations generated by earthquake shaking could impart a destabilizing force sufficient to temporarily reduce the factor of safety of a slope below 1, leading to sliding episodes and the accumulation of permanent, downslope sliding displacement. The original Newmark procedure models the sliding mass as a rigid block and utilizes two parameters: the yield acceleration (k_y, the acceleration in units of g that initiates sliding for the slope) and the acceleration-time history of the rigid foundation beneath the sliding mass. A sliding episode begins when the acceleration exceeds k_y and continues until the velocity of the sliding block and foundation again coincide. The relative velocity between the rigid block and its foundation is integrated to calculate the relative sliding displacement for each sliding episode and the sum of the displacements for each sliding episode represents the cumulative sliding displacement (Figure 1).

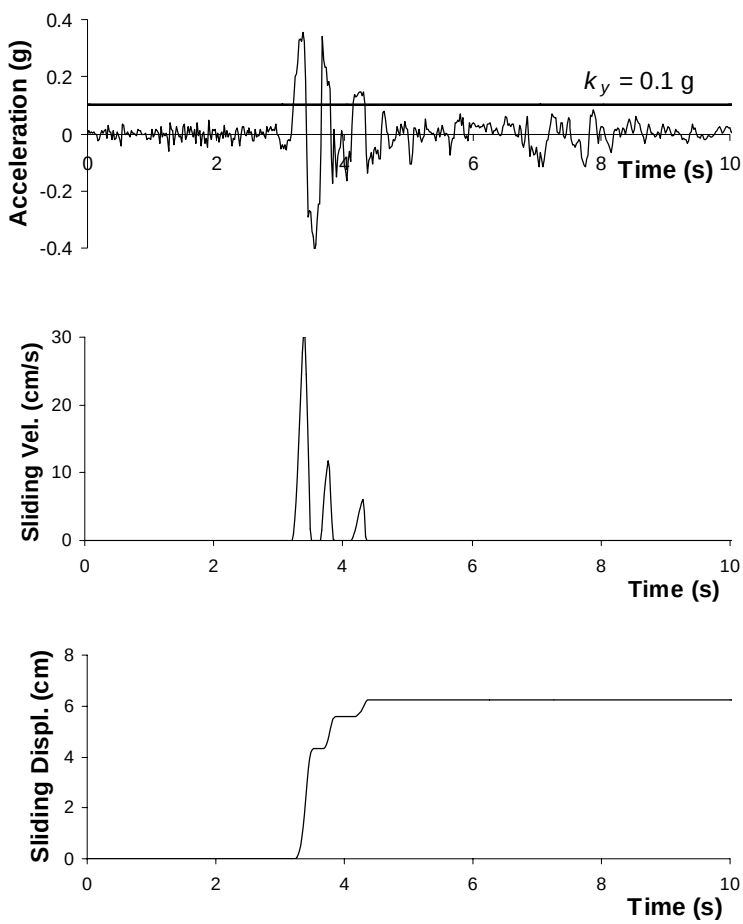

Figure 1. Acceleration-time history, sliding velocity-time history, and sliding displacement-time history for a rigid sliding block and k_y = 0.1.

The original rigid sliding block procedure is applicable to thin, veneer slope failures. This failure mode is common in natural slopes, while deeper sliding surfaces are common in engineered earth structures. The sliding block displacement methodology has been extended to account for the deformable response of deeper sliding masses in earth structures (e.g., Seed and Martin 1966, Makdisi and Seed 1978, Bray and Rathje 1998), and to account for the coupled interaction between sliding and dynamic responses (Rathje and Bray 1999, 2000). Nonetheless, for natural slopes, rigid sliding block analysis is the most common analytical procedure used to predict the potential for earthquake-induced landslides and will be the focus of this work.

The magnitude of sliding displacement is strongly affected by the characteristics (i.e., intensity, frequency content, duration) of the earthquake ground motion. Various researchers have proposed models that predict sliding displacement as a function of ground motion parameters (e.g., peak ground acceleration, Arias intensity) and site parameters (k_y, site period). These displacement models work in a similar way to ground motion prediction models in that displacement is predicted as a function of the given input parameters. The displacement models have significant aleatory variability (large standard deviation, σ_{ln}, for the predicted displacement) such that a large range of displacements is predicted for the given input parameters. In addition to this variability, earthquake ground motions also display significant aleatory variability. Yet, current evaluation procedures that use sliding block displacements to evaluate the potential for slope instability typically are based on a deterministic approach or a pseudo-probabilistic approach, in which the variabilities in the expected ground motion and predicted displacement are either ignored or not treated rigorously. Thus, there is no concept of the actual hazard associated with the computed displacement.

A fully probabilistic assessment of sliding displacement can rigorously account for the aleatory variability in the earthquake ground motion prediction and in the sliding displacement prediction. The product of a probabilistic assessment of sliding displacement is a displacement hazard curve, which provides the annual rate of exceedance, λ, for a range of displacement levels. The computation of a displacement hazard curve requires a displacement model that predicts displacement as a function of ground motion and site parameters, the aleatory variability (σ_{ln}) for the displacement model, and the hazard curve for the ground motion parameter(s) used in the displacement model.

The aleatory variability in the sliding displacement prediction can be significantly reduced if more than one ground motion parameter is used in the displacement prediction equation. In this case, a vector hazard approach is required (Bazzurro and Cornell 2002, Yegian et al. 1991a). Bazzurro and Cornell (2002) demonstrated the vector approach by computing hazard curves for the inter-story drift of a 20-story building, a system whose response is affected by the spectral acceleration at its first and second modal frequencies. For the vector hazard approach, the only additional information required is the correlation between the ground motion parameters. The vector hazard approach is potentially important for the permanent deformations of slopes because the aleatory variability of the predicted displacement can be significantly reduced when more than one ground motion parameter is used.

This report presents a framework for developing probabilistic seismic hazard curves for sliding displacement based on the work of Bazzurro and Cornell (2002), develops the appropriate empirical models that predict sliding displacement as a function of different ground motion parameters, generates the required correlation information for the ground motion vectors used to predict sliding displacement, and applies the probabilistic framework to develop displacement

hazard curves. Details regarding this work can be found in Rathje and Saygili (2008) and Saygili and Rathje (2008).

PROBABILISTIC FRAMEWORK FOR SLIDING DISPLACEMENTS

Various deterministic and probabilistic methodologies are used in practice to predict the sliding displacement of a slope (Figure 2). A deterministic approach first requires the selection of a design earthquake scenario, defined by the magnitude, *M*, and distance, *R*. This scenario may be the maximum magnitude event on the closest fault, or multiple scenarios may be specified (e.g., a larger magnitude event at moderate distance and a smaller magnitude event at closer distance). After selection of the earthquake scenario(s), the ground motion (*GM*) is predicted based on a ground motion prediction model and a selected number of standard deviations above the median (ε_{GM}). The selection of ε_{GM} is somewhat arbitrarily set to 0 or 1, and its presence inherently introduces some probability into the analysis, despite it being considered "deterministic". Finally, the displacement is predicted using the yield acceleration of the slope (k_y) and the predicted ground motion (*GM*). The displacement prediction may be derived from a displacement predictive model or chart (e.g., Makdisi and Seed 1978, Franklin and Chang 1977), or through a more rigorous procedure that involves selecting a suite of motions to fit the *GM* and computing the displacement for each motion. Again, the number of standard deviations above the median displacement prediction (ε_D) must be selected, which is used to account for the variability into the computed displacement.

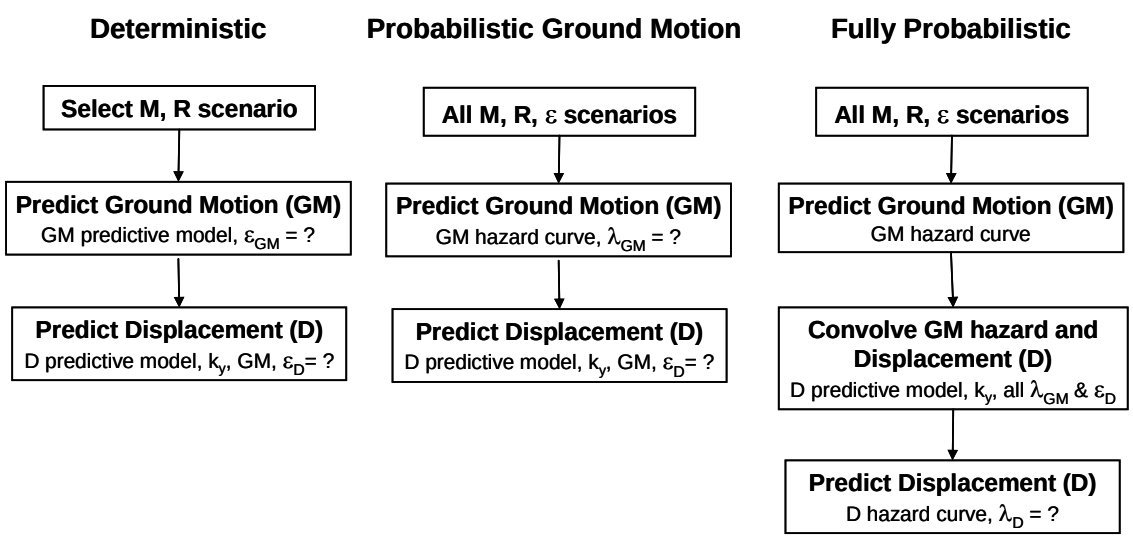

Figure 2. Various methodologies for predicting sliding displacements

The variability in the ground motion can be more explicitly considered in this analysis through a probabilistic assessment of the ground motion (Figure 2). Here, a seismic hazard curve is developed for the ground motion parameter of interest, and this curve defines the mean annual rate of exceedance (λ_{GM}) for different levels of ground motion. This hazard curve accounts for all potential earthquake/ground motion scenarios (*M*, *R*, and ε_{GM}), the probability of occurrence of each scenario, and the probability that a ground motion level is exceeded given the scenario.

The design ground motion is derived from the hazard curve through the selection of an acceptable $\lambda_{GM,}$ and this ground motion level is used in the prediction of sliding displacement. However, the treatment of the variability in the sliding displacement remains ambiguous.

The variability in the ground motion and sliding displacement both can be taken into account through a fully probabilistic analysis (Figure 2). This analysis convolves the full ground motion hazard curve, which includes all of the ground motion variability, with the displacement model and all of its variability. The uncertainties in the properties of the slope (e.g., k_y) are not taken into account, but could also be incorporated. The result is a displacement hazard curve that provides the mean annual rate of exceedance (λ_D) for different levels of sliding displacement. This curve is well-suited for making engineering decisions, as it provides the probability of exceedance for a damage measure of the slope (i.e. sliding displacement) given all of the ground motion and sliding displacement variabilities. This fully probabilistic methodology is described in detail below.

Scalar Hazard for Ground Motion

In traditional probabilistic seismic hazard analysis (PSHA), a relationship is developed between the ground motion level (e.g., peak ground acceleration, PGA) and its mean annual rate of exceedance (λ or MRE). This calculation is based on all of the faults in the area, all of the potential earthquake scenarios on each source (i.e., magnitude recurrence, earthquake location, site-to-source distance), and a ground motion prediction model that predicts the ground motion as a function of the earthquake scenarios (magnitude, distance, etc.). This calculation can be displayed for one source as:

$$\lambda_{GM}(z) = MRE_{GM}(z) = \lambda_o \cdot \int_m \int_r P\left[GM > z \middle| m, r\right] f_M(m)\, f_R(r) \cdot dmdr \qquad (1)$$

where $\lambda_{GM}(z)$, or $MRE_{GM}(z)$, is the mean annual rate that the ground motion parameter (GM) exceeds a given level (z), λ_o is the annual rate of earthquakes greater than the minimum magnitude (also called the activity rate), m is magnitude, r is distance, and $f_M(m)$ and $f_R(r)$ are the probability density functions for m and r, respectively. $P\left[GM > z \middle| m, r\right]$ is the probability that the ground motion level is exceeded for the given earthquake scenario (m and r). This probability is derived from the ground motion prediction relationship and its standard deviation ($\sigma_{\ln}$). Ground motion prediction relations assume the ground motion to be log-normally distributed, and thus the probability of exceedance calculation can be simply performed using the standard normal distribution of the natural log of the ground motion. To develop a hazard curve, equation (1) is used with a suite of ground motion levels (z = 0.05 g, 0.1 g, etc.) to produce a relationship between λ and z.

As a hazard curve is analogous to a complementary cumulative density function, its derivative represents the mean annual rate density of the ground motion ($MRD_{GM}(z)$, Bazzurro and Cornell 2002) and is analogous to a probability density function:

$$MRD_{GM}(z) = \frac{d}{dz}\left[MRE_{GM}(z)\right] = \lambda_o \cdot \int_m \int_r f_{GM}(z \middle| m, r) \cdot f_M(m) \cdot f_R(r) \cdot dmdr \qquad (2)$$

Here, $f_{GM}(z|m,r)$ is the standard lognormal probability density function given by:

$$f_{GM}(z|m,r) = \frac{1}{z \cdot \sigma_{\ln GM} \cdot \sqrt{2\pi}} \cdot \exp\left(\frac{-(\ln z - \mu_{\ln GM})^2}{2 \cdot \sigma_{\ln GM}^2} \right) \quad (3)$$

with the mean ($\mu_{\ln GM}$) and standard deviation ($\sigma_{\ln GM}$) in natural log units and derived from a ground motion prediction relationship.

Scalar Hazard for Sliding Displacement

Similar to the probabilistic evaluation of the ground motion hazard, the goal of a probabilistic evaluation of permanent sliding displacement is a relationship between sliding displacement level (D) and its mean annual rate of exceedance (λ_D or MRE_D). This computation is represented by:

$$\lambda_D(x) = MRE_D(x) = \int P\left[D > x | GM = z\right] \cdot MRD_{GM}(z) \cdot dz \quad (4)$$

where $\lambda_D(x)$, or $MRE_D(x)$, is the mean annual rate that the sliding displacement (D) exceeds a given level (x), $P\left[D > x | GM = z\right]$ is the probability that the displacement level x is exceeded given the ground motion level z (i.e., $GM = z$), $MRD_{GM}(z)$ is the mean rate density for the ground motion, and represents the probability of occurrence of ground motion level z. $MRD_{GM}(z)$ is derived from the derivative of the hazard curve (equation 2). To use equation (4) to develop a displacement hazard relationship, the only additional information required beyond a ground motion hazard curve is the displacement relation that predicts D as a function of a ground motion parameter and that relation's associated standard deviation ($\sigma_{\ln}$).

To compute a displacement hazard curve, equation (4) is used with a suite of displacement levels (x) to produce a relationship between λ_D and displacement level. Because only one ground motion parameter is used in (4), this is considered a scalar probabilistic seismic hazard analysis. This framework is similar to the framework of DelGaudio et al. (2003), which considered the probability of landslide failures based on probabilistic evaluations of sliding displacement.

Vector Hazard for Sliding Displacement

If the permanent sliding displacement depends heavily on two ground motion parameters (e.g., an intensity and frequency content parameter, see accompanying paper by Saygili and Rathje 2007), a vector hazard approach is required (Bazzurro and Cornell 2002). In this case, the displacement hazard calculation becomes:

$$\lambda_D(x) = MRE_D(x) = \int\int P\left[D > x | GM1 = z, GM2 = y\right] \cdot MRD_{GM1,GM2}(z,y) \cdot dz \cdot dy \quad (5)$$

where $P\left[D > x | GM1 = z, GM2 = y\right]$ is the probability that the displacement level x is exceeded given the joint occurrence of two ground motion parameters, *GM1* and *GM2*,

$MRD_{GM1,GM2}(z,y)$ is the joint mean rate density of *GM1* and *GM2*, and represents the joint probability of occurrence of ground motion levels *GM1=z* and *GM2=y*. Again, the displacement probability is determined from the predictive relationship for *D*, which in this case is a function of two ground motion parameters, *GM1* and *GM2*. The added complexity comes from the joint *MRD* for *GM1* and *GM2*. The joint *MRD* is given by (Bazzurro and Cornell 2002):

$$MRD_{GM1,GM2}(z,y) = \lambda_o \cdot \int_m \int_r f_{GM1,GM2}(z,y|m,r) \cdot f_M(m) \cdot f_R(r) \cdot dm \cdot dr \tag{6}$$

where $f_{GM1,GM2}(z,y|m,r)$ is the joint probability density function for *GM1* and *GM2* given *m* and *r*. This probability density function can be written in conditional form (Bazzurro and Cornell 2002):

$$f_{GM1,GM2}(z,y|m,r) = f_{GM1}(z|m,r) \cdot f_{GM2|GM1}(y|z,m,r) \tag{7}$$

The first term in this equation, $f_{GM1}(z|m,r)$, is the probability density function for *GM1* conditional on *m* and *r* (same as scalar PSHA, equation 3) and is derived from the ground motion prediction equation for *GM1*. However, the second term, $f_{GM2|GM1}(y|z,m,r)$, is the probability density function for *GM2* conditional on *m*, *r*, <u>and</u> a *GM1* value of *z*.

The conditional probability density function for *GM2* in equation (7) is still assumed to be lognormal (Bazzurro and Cornell 2002) and can be described with the probability density function in equation (3). However, the probability density function utilizes modified values of the mean (μ_{ln}) and standard deviation ($\sigma_{\ln}$) that are based on the mean values for ln*GM1* and ln*GM2*, the standard deviations of ln*GM1* and ln*GM2*, the value of *GM1* = *z*, and the correlation (ρ) between parameters *GM1* and *GM2*. Specifically (Benjamin and Cornell 1970):

$$\mu_{\ln GM2|z,m,r} = \mu_{\ln GM2|m,r} + \rho \frac{\sigma_{\ln GM2|m,r}}{\sigma_{\ln GM1|m,r}} \cdot \left(\ln z - \mu_{\ln GM1|m,r}\right) \tag{8}$$

$$\sigma_{\ln GM2|z,m,r} = \sigma_{\ln GM2|m,r} \cdot \sqrt{1-\rho^2} \tag{9}$$

For equations (8) and (9), the ground motion prediction equations for *GM1* and *GM2* provide the parameters $\mu_{\ln GM1|m,r}$, $\mu_{\ln GM2|m,r}$, $\sigma_{\ln GM1|m,r}$, and $\sigma_{\ln GM2|m,r}$. Thus, the only additional information required is the correlation coefficient, ρ.

In summary, if only one ground motion parameter is used to predict the permanent sliding displacement, equation (4) is used to compute the displacement hazard. The information required for this analysis is the displacement predictive equation, its standard deviation ($\sigma_{\ln}$), and the hazard curve for the ground motion parameter. If two ground motion parameters are required to predict the sliding displacement, equations (5) through (9) are used to compute the displacement hazard. The information required for this analysis is the sliding displacement predictive equation, its standard deviation, and the MRD for the vector of ground motion parameters. The MRD calculation requires the predictive equations for the ground motion

parameters, the standard deviations for these relationships, and the correlation coefficient between the ground motion parameters.

SLIDING DISPLACEMENT MODELS APPROPRIATE FOR PROBABILISTIC ANALYSIS

Many researchers have proposed models that predict rigid block sliding displacement as a function of ground motion parameters (e.g., peak ground acceleration, Arias intensity) and site/slope parameters (k_y, site period). Newmark (1965) computed rigid block displacements for four earthquake motions and showed that displacement was a function of k_y, peak ground acceleration (*PGA*), and peak ground velocity (*PGV*). Franklin and Chang (1977), Ambraseys and Menu (1988), Yegian et al. (1991), and Ambraseys and Srbulov (1994) developed charts and/or predictive equations for rigid sliding block displacements using different ground motion datasets. However, these models were developed based on somewhat limited datasets and the resulting predictive equations displayed very large variability ($\sigma_{ln} > 1.0$).

Recent research has used larger ground motion datasets to develop displacement predictive models and developed better estimates of the variability (σ_{ln}) in the predictions. Jibson et al. (2000) developed a predictive model for rigid block conditions using 555 components of ground motion from 280 recording stations from 13 earthquakes. The Jibson model is a function of the Arias intensity (I_a) of the ground motion and k_y of the slope, and the standard deviation (σ_{ln}) for their proposed equation is 0.86. Watson-Lamprey and Abrahamson (2006) developed a model for rigid block displacement using a large dataset consisting of 6,158 recordings scaled with seven different scale factors and computed for three values of yield acceleration. Their displacement model is a function of various parameters including *PGA*, spectral acceleration at a period of 1 second ($Sa_{T=1s}$), root mean square acceleration (A_{RMS}), k_y, and the duration for which the acceleration-time history is greater than the yield acceleration (Dur_{ky}). However, a standard deviation for the predictive model was not presented, although this information was available for preliminary versions of the model and ranged from 0.3 to 0.7 in natural log space (Abrahamson, personal communication).

Bray and Travasarou (2007) presented a predictive relationship for earthquake-induced displacements of rigid and deformable slopes. Displacements were calculated using the equivalent-linear, fully–coupled, stick-slip sliding model of Rathje and Bray (1999, 2000). 688 earthquake records (2 orthogonal components per record) obtained from 41 earthquakes were used to compute displacements for ten values of k_y and eight site geometries (i.e., fundamental site periods, T_s). Displacements for the two components of orthogonal motion were averaged and values less than 1 cm were set equal to zero because they were assumed to be of no engineering significance. The model input parameters include k_y, the initial fundamental period of the sliding mass (T_s), the magnitude of the earthquake (M_w), and the spectral acceleration at a degraded period equal to $1.5T_s$, called $S_a(1.5Ts)$. When considering shallow, rigid sliding surfaces, $S_a(1.5Ts)$ is taken as *PGA* and $T_s = 0$. The standard deviation (σ_{ln}) for the predictive model is 0.66.

Of the current models, the Jibson et al. (2000) and Bray and Travasarou (2007) models are the most appropriate for PSHA because they were developed using large datasets and rigorous regression techniques, and they provide estimates of the σ_{ln} of the displacement prediction. Yet, the Jibson et al. (2000) model has significant aleatory variability (σ_{ln}) such that a large range of displacements are predicted for the given ground motion and site/slope parameters. The σ_{ln} for the Bray and Travasarou (2007) model is smaller than for Jibson et al.

(2000); however, it does not take advantage of multiple ground motion parameters to predict the displacement and further reduce σ_{ln}. The goal of this study is to develop rigid block displacement predictive equations that utilize multiple ground motion parameters in an effort to reduce the aleatory variability (σ_{ln}). These displacement predictive equations can be used to develop hazard curves for sliding displacement using either the scalar or vector approach.

FRAMEWORK FOR DISPLACEMENT MODEL DEVELOPMENT

Rigid sliding block displacements were computed using the rigid sliding block programs developed by Jibson and Jibson (2003, 2006). The computed displacement values were then used to develop predictive relationships for displacement as a function of k_y and different combinations of ground motion parameters, with the goal of identifying the combination(s) of ground motion parameters that produce the smallest variability in the prediction of sliding displacement. The developed displacement models can be used to compute hazard curves for earthquake-induced permanent displacement, can be used as predictive tools for deterministic earthquake scenarios, or can be used to rapidly predict the likelihood of earthquake-induced landslides after an earthquake using recorded ground motions.

Ground Motion Database

Variability in the expected ground motion is the biggest contributor to the variability in the displacement prediction; thus, using a large, high-quality dataset of strong motion records is essential to developing a robust displacement model. Currently the number of available records is considerable and one significant dataset is readily available from the Next Generation Attenuation (NGA) strong motion database of the Pacific Earthquake Engineering Research Center <http://peer.berkeley.edu/nga>

The initial dataset included motions from earthquakes ranging from M_w = 5 to 7.9 and distances from 0.1 to 100 km. Motions recorded at soft soil sites, on the crest or abutments of dams, underground, not at the ground floor of a building, or in buildings larger than 4 stories were removed from the database. Additionally, motions with high-pass filter corner frequencies larger than 0.25 Hz or low-pass filter corner frequencies less than 10 Hz were removed. The resulting dataset included 2,383 motions. Rigid sliding block displacements were computed for k_y values of 0.05, 0.1, 0.2, and 0.3, which encompasses typical values for earth slopes. For each motion, displacements were calculated for positive and negative polarities, with the largest displacement used for the model development. Displacements computed from orthogonal components recorded at the same station during the same earthquake were treated as separate data points for the model.

Approximately 25% of the initial ground motion dataset had values of *PGA* less than 0.05 g, and thus these motions do not predict any displacement for the k_y values used. To further populate the database at larger values of *PGA*, displacements were also calculated for each motion scaled by factors of 2.0 and 3.0. To ensure that unreasonable *PGA* values were not used when scaling the motions, the motions were capped at *PGA* = 1.0 g. However, regressions were also performed using motions up to *PGA* = 2.0 g, and similar results were obtained. The final displacement dataset when capping *PGA* = 1.0 g included approximately 14,000 non-zero displacements. The distribution of records in the final ground motion dataset in terms of earthquake magnitude, closest distance, and various ground motion parameters is given in Fig. 3.

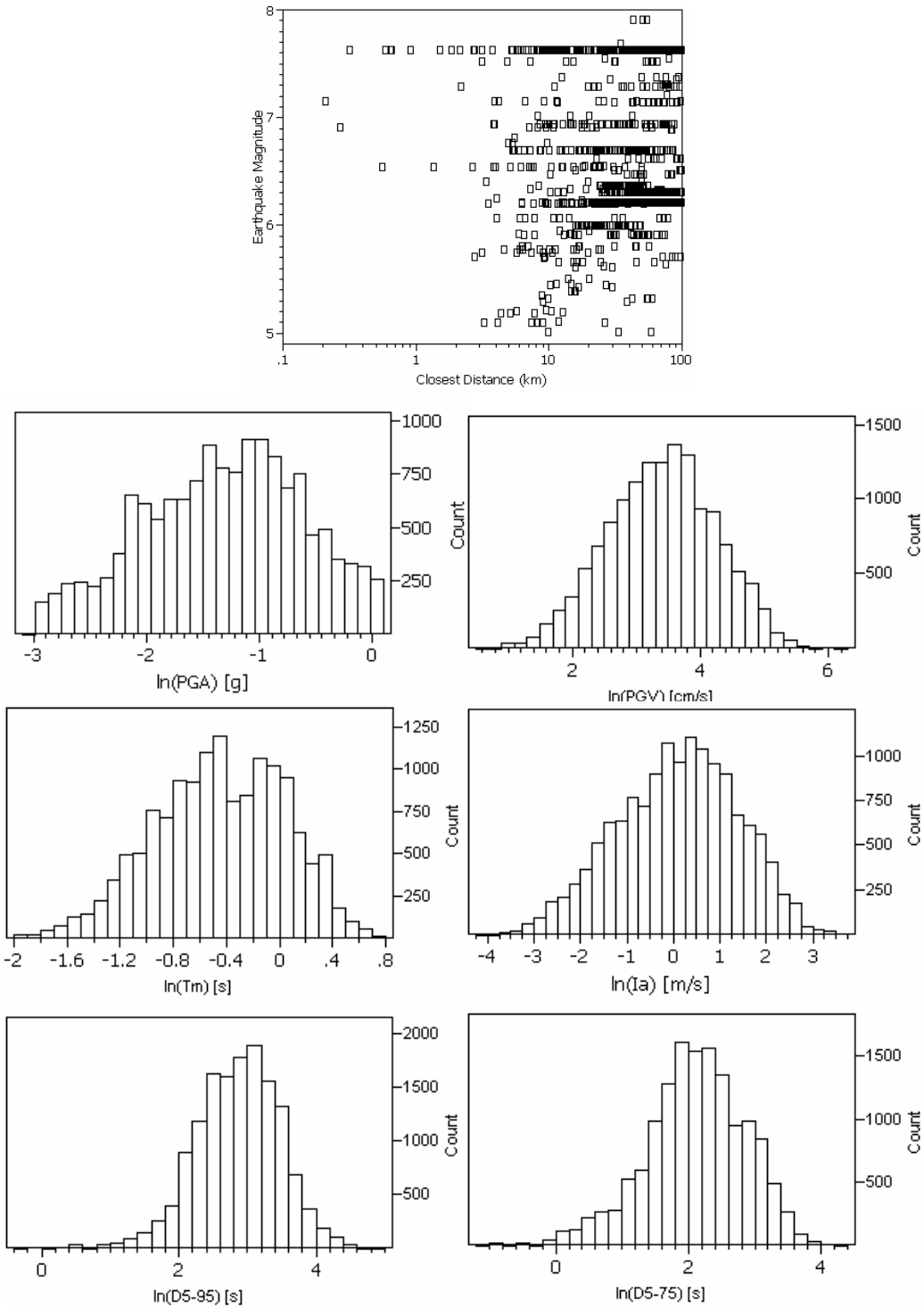

Figure 3: Distribution of records used in displacement model in terms of earthquake magnitude, closest distance, and various ground motion parameters

Ground Motion Parameter Selection

The sliding displacement of earth slopes is a function of various features of the expected ground motion such as intensity, frequency content, and duration of shaking. These key ground

motion characteristics cannot be easily quantified in a single ground motion parameter; instead, an optimal vector of ground motion parameters is employed. The ground motion parameters considered in this study are (Figure 3): peak ground acceleration (*PGA* in g), peak ground velocity (*PGV* in cm/s), mean period (T_m in seconds), Arias intensity (I_a in m/s), and two definitions of duration based on the build-up of Arias Intensity ($D_{5\text{-}95}$ and $D_{5\text{-}75}$ in seconds).

The selection of optimal ground motion parameters is based predominantly on the 'efficiency' criterion proposed by Cornell and Luco (2001). The term 'efficiency' is related to the variability of the random error obtained from the regression. In this sense, ground motion parameters that produce less variability ($\sigma_{\ln}$) in the displacement prediction are considered more efficient. Cornell and Luco (2001) also specify a 'sufficiency' criterion for predictive equations for engineering demand parameters, such that the selected ground motions can sufficiently predict the engineering demand parameter without the need for specifying the earthquake magnitude or site-to-source distance.

Consider the prediction of sliding displacement for a rigid slope with k_y = 0.05. The efficiency of different scalars and vectors of ground motion parameters to predict the displacement of this slope initially can be tested by fitting the following 2nd-order polynomials to the calculated displacements:

$$\ln(D) = \alpha_1 + \alpha_2 \ln(GM) + \alpha_3 \left(\ln(GM)\right)^2 \qquad \text{(SCALAR)} \quad (10a)$$

$$\ln(D) = \alpha_1 + \alpha_2 \ln(GM1) + \alpha_3 \left(\ln(GM1)\right)^2 + \alpha_4 \ln(GM2) + \alpha_5 \left(\ln(GM2)\right)^2 \qquad \text{(VECTOR)} \quad (10b)$$

For the vectors of ground motion parameters, *PGA* was used as *GM1* and coupled with the remaining parameters. *PGA* was explicitly used as *GM1* in the vector because when it is compared with k_y it provides a direct assessment of whether the displacement will be greater than zero (i.e., if $PGA > k_y$, then $D > 0$).

Sliding displacements for k_y = 0.05 are plotted versus the six considered ground motion parameters in Figure 4, along with the curves fit using equation (10). Based on the standard deviations of the predictions shown in Figure 4, I_a is the most efficient ground motion parameter ($\sigma_{\ln}$ = 0.97), followed by *PGA* ($\sigma_{\ln}$ = 1.20) and *PGV* ($\sigma_{\ln}$ = 1.39). The frequency content and duration ground motion parameters (T_m, $D_{5\text{-}95}$, and $D_{5\text{-}75}$) display weak correlation with sliding displacement. This result is due to the fact that intensity predicts the onset of sliding, and thus initially is more important than either frequency content or duration in predicting sliding displacement.

The computed values of standard deviation for scalar and vector regressions using the various ground motion parameters and different values of k_y are given in Figure 5. Considering the standard deviations for the scalar models, I_a is the most efficient scalar ground motion parameter for k_y = 0.05, while for $k_y \geq 0.1$ *PGA* is the most efficient scalar parameter. These results are similar to those of Bray and Travasarou (2007). *PGA* is generally the most efficient because its value in relation to k_y indicates (1) whether the motion is strong enough to induce sliding and (2) the intensity of the induced sliding velocity and thus sliding displacement (Figure 1). I_a is slightly more efficient at very low k_y because in these cases a large portion of the acceleration-time history is sampled during the displacement calculation and I_a provides information about the intensity, frequency content, and duration of the motion. The scalar

standard deviations in Figure 5 generally increase with increasing values of k_y, particularly for I_a and *PGV*. Again, this result is caused by the fact that the portion of an acceleration-time history sampled by the displacement calculation varies with k_y. Little of the motion is sampled at large k_y, such that the additional information provided by parameters such as I_a and *PGV* does not improve the displacement prediction.

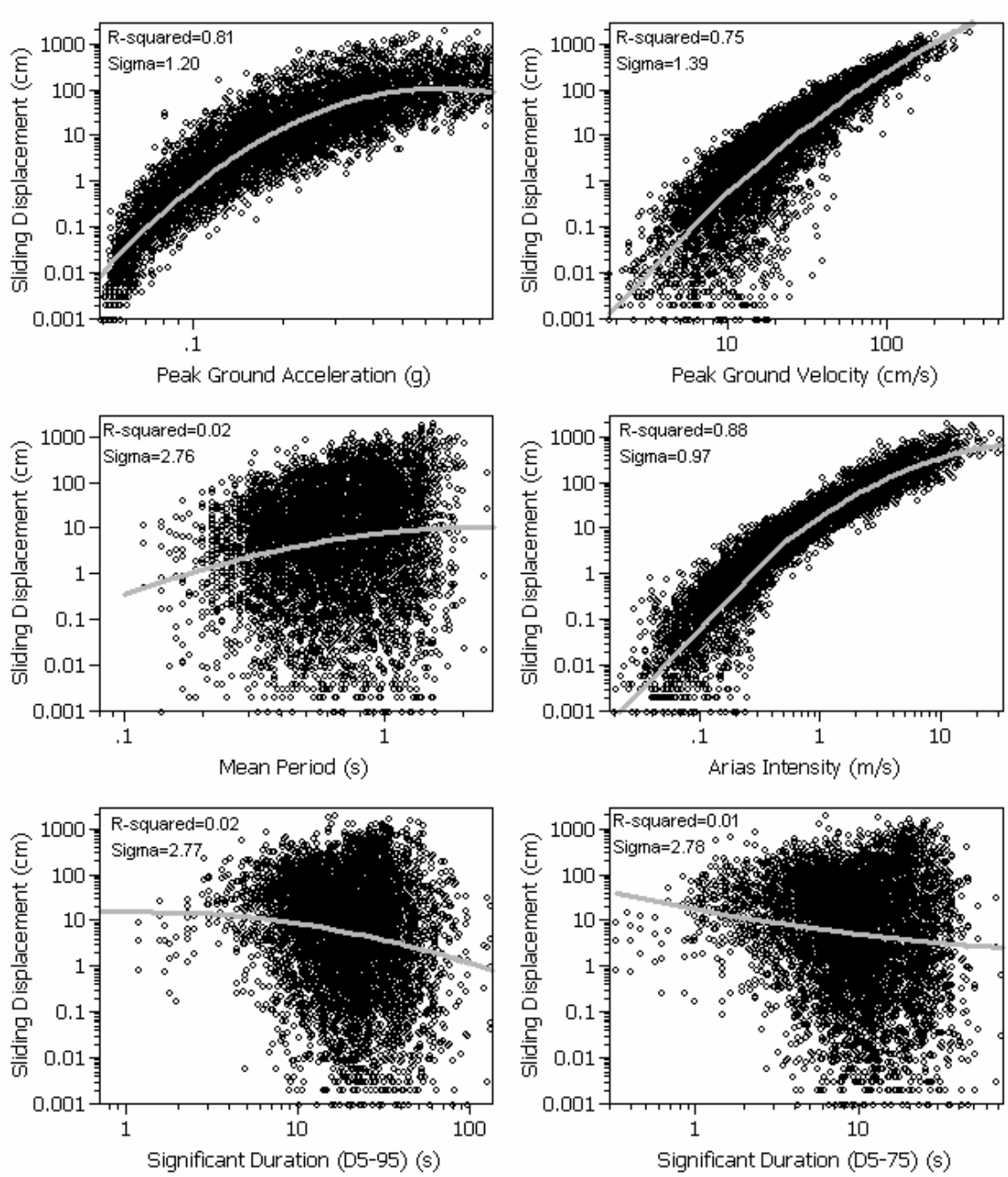

Figure 4: Regression of sliding displacement for quantifying scalar efficiencies of different ground motion parameters (k_y = 0.05)

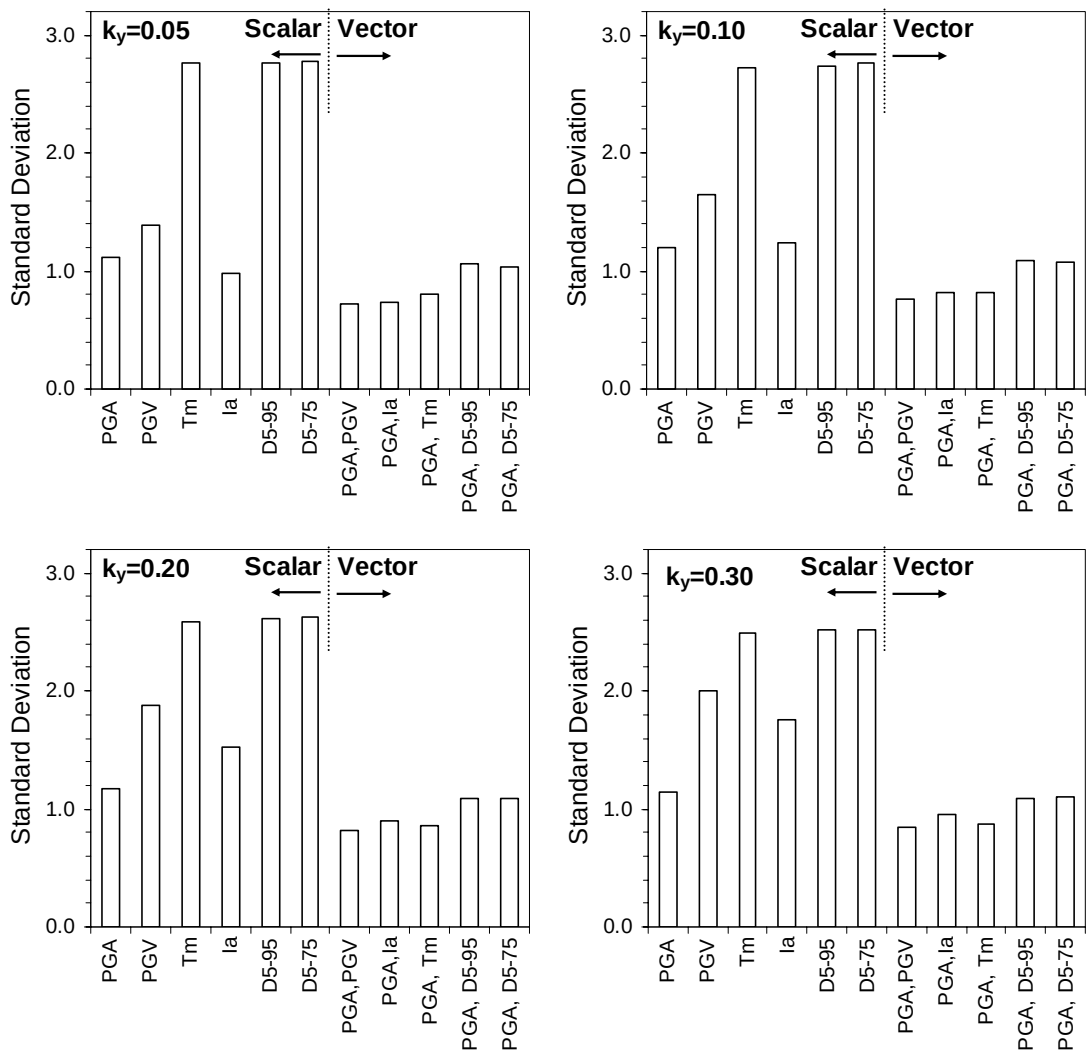

Figure 5: Standard deviation of regression models for sliding displacement for different values of k_y and different ground motion parameters

The vector standard deviations in Figure 5 indicate that the efficiency significantly improves when vectors of two ground motion parameters are used. Using more than one ground motion parameter enables the model to capture additional significant features of the motion that affect sliding displacement (e.g., intensity <u>and</u> frequency content) rather than address only one feature (e.g., intensity <u>or</u> frequency content). From the efficiency point of view, the most inefficient vector model is more efficient than the most efficient scalar model (Figure 5). *PGA* and I_a are the two most efficient scalar ground motion parameters, yet the combination of *PGA* and *PGV* is the most efficient vector model. This result is due to the multicollinearity between *PGA* and I_a. That is, both ground motion parameters have significant explanatory power, yet they overlap so significantly that they essentially provide almost the same information to the regression. Correlation coefficients between parameters are helpful in detecting multicollinearity. The correlation coefficient between *PGA* and I_a ($\rho_{PGA,Ia}$) is approximately 0.8 (see next section), while $\rho_{PGA.PGV}$ is about 0.6. A smaller value of ρ indicates that the two parameters provide more complementary information about the ground motion, and consequently the combination of these

ground motion parameters captures additional information that leads to a smaller standard deviation in the displacement prediction.

The (*PGA*, *PGV*) and the (*PGA*, I_a) models are the two most efficient vector models for relatively weaker slopes ($k_y < 0.1$); while the (*PGA*, *PGV*) model and the (*PGA*, T_m) model are the most efficient vector models for relatively stronger slopes ($k_y \geq 0.1$). Nonetheless, all three of these vector models (*PGA*, *PGV*; *PGA*, I_a; and *PGA*, T_m) have very similar standard deviations, and these models are more efficient than either of the *PGA*-duration models (Figure 5). The concept of efficiency will be used to assess the final displacement models developed in the next sections.

If the resulting displacement relationship for a given scalar and/or vector of ground motions is independent of earthquake magnitude and distance, then the 'sufficiency' criterion is satisfied (Luco and Cornell 2001). In that case, the seismic hazard is conditioned only on the ground motion parameter(s). This allows decoupling of the seismic hazard and system response evaluation, and significantly simplifies the computational effort. The 'sufficiency' of scalar ground motion parameters and vectors of ground motion parameters is addressed for the final regression models, given in the next sections.

SCALAR PREDICTIVE MODEL

Functional form of the predictive equation

To develop a generalized predictive model that is appropriate for different values of k_y, a functional form that encompasses the ratio of k_y to *PGA* was employed. The k_y/PGA term allows zero displacements to be explicitly assigned when k_y/PGA is greater than 1.0, and non-zero displacements assigned otherwise. The displacements show a higher order shape with respect to k_y/PGA in semi-log space. Up to 5th order terms were considered for k_y/PGA using:

$$\ln D = \beta_1 + \beta_2\left(\frac{k_y}{PGA}\right) + \beta_3\left(\frac{k_y}{PGA}\right)^2 + \beta_4\left(\frac{k_y}{PGA}\right)^3 + \beta_5\left(\frac{k_y}{PGA}\right)^4 + \beta_5\left(\frac{k_y}{PGA}\right)^5 \tag{11}$$

The selection of the necessary higher order terms was based on the bias in the displacement predictions when using 3rd, 4th, and 5th order polynomials in equation (11) Generally, the inclusion of higher order terms did not significantly change the standard deviation of the predictions.

Figure 6 plots the mean residuals for the 3rd, 4th, and 5th order polynomial equations computed for different k_y/PGA bins. While the mean residuals for the full data set are very close to zero, Figure 6 shows that for each functional form the mean residuals vary with k_y/PGA. This trend generally indicates that the data vary with a higher order than that used in the regression. For the 4th and 5th order polynomials, the binned mean residuals in Figure 6 are generally within ±0.1 (in natural log units) for $k_y/PGA \leq 0.75$, indicating biases less than 10%. Each functional form reveals noteworthy bias at $k_y/PGA > 0.75$. However, at these levels of k_y/PGA, the predicted displacements are generally small and the level of bias is not of engineering significance. To minimize the potential bias in the model but to maintain a relatively simple equation, the 4th order polynomial functional form was selected for use in the developed predictive models.

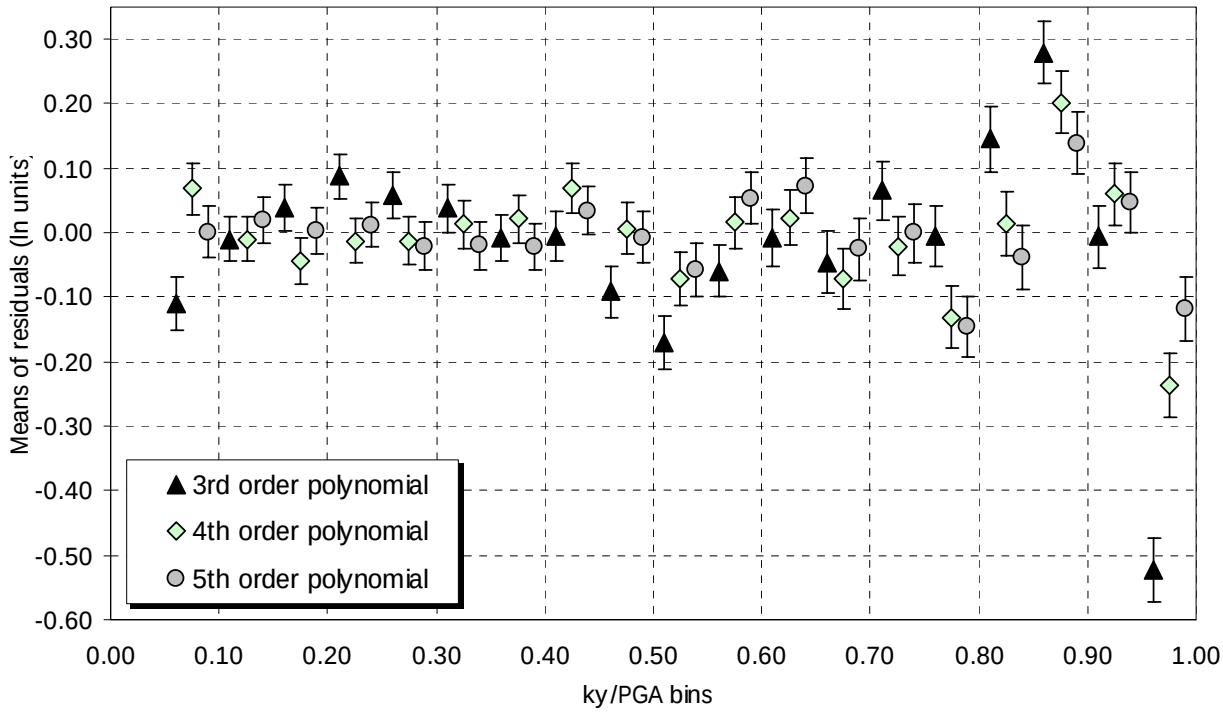

Figure 6: Mean of residuals versus k_y/PGA for different functional forms of the regression model

Scalar predictive equation

Using the 4th order polynomial in equation (11), an initial regression was performed. The residuals ($\ln D_{observed} - \ln D_{predicted}$) for the resulting model varied with *PGA;* thus, an additional *PGA* term was included in the scalar predictive equation. The resulting scalar displacement model using only one ground motion parameter (*PGA*) is;

$$\ln D = a_1 + a_2\left(\frac{k_y}{PGA}\right) + a_3\left(\frac{k_y}{PGA}\right)^2 + a_4\left(\frac{k_y}{PGA}\right)^3 + a_5\left(\frac{k_y}{PGA}\right)^4 + a_6 \ln(PGA) + \varepsilon\sigma_{\ln} \qquad (12)$$

where D is the sliding displacement (cm), k_y is the yield acceleration coefficient in units of g, *PGA* is the peak ground acceleration in units of g, $\sigma_{\ln}$ is the standard deviation in natural log units, and ε is the standard normal variate with zero mean and unit standard deviation. The coefficients a_1 through a_6 and their standard errors are given in Table 1, along with the standard deviation ($\sigma_{\ln}$). To calculate the median displacements using equation (12), ε is set to zero, while for one standard deviation above the median, ε is equal to +1, etc.

Figure 7 shows all of the displacement data versus k_y/PGA, along with the predicted median displacement from equation (12) for *PGA* values of 0.1 g and 0.5 g. By including the additional effect of *PGA*, Figure 7 shows that for a given value of k_y/PGA, the displacement increases by more than a factor of 3 when the *PGA* increases from 0.1 to 0.5 g. Adding an additional *PGA* term in the model reduced the total standard deviation from 1.20 to 1.13. Nonetheless, this standard deviation is very large and thus vectors of ground motion parameters were considered.

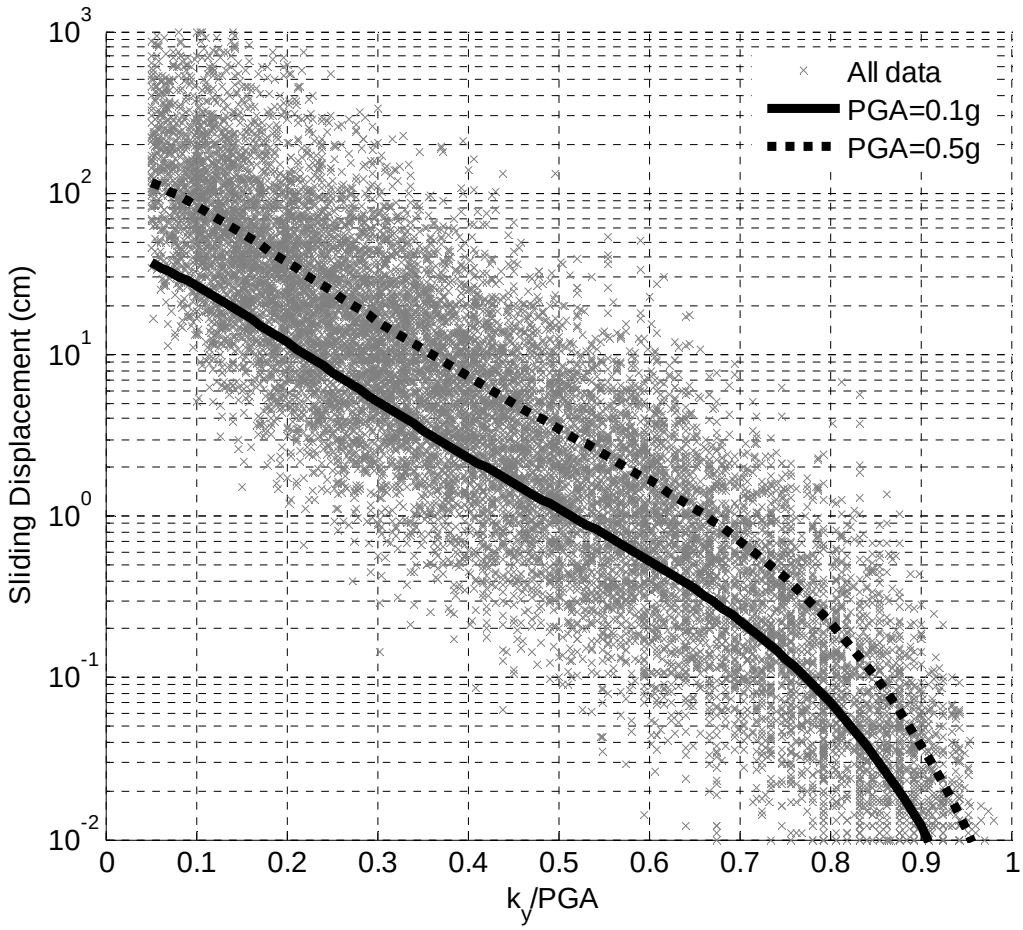

Figure 7: Rigid sliding block displacement versus k_y/PGA

Vector predictive equations

In an effort to reduce the standard deviation of the predicted sliding displacements, various ground motion parameters were considered for inclusion in the predictive model. As noted previously, these parameters are *PGV*, I_a, T_m, $D_{5\text{-}75}$, and $D_{5\text{-}95}$, and they represent intensity, frequency content, and duration parameters.

To investigate which ground motion parameters have the biggest effect on the computed displacements, the means of the residuals ($\ln D_{obs} - \ln D_{pred}$) with respect to equation (12) are plotted versus each of the omitted ground motion parameters in Figure 8. It is clear that each of the omitted ground motion parameters affects sliding displacement because the residuals increase with increasing values of each parameter. The residuals vary most strongly with T_m and *PGV*, both of which represent measures of frequency content. A similar result was found by Ambraseys and Srbulov (1994). Frequency content affects sliding displacement because motions with more long period energy have longer sliding episodes that lead to more displacement. The residuals also vary with I_a, $D_{5\text{-}75}$, and $D_{5\text{-}95}$, although not as strongly as with T_m and *PGV*.

Table 1: Model parameters and standard errors of the model parameters (in parentheses) for the proposed sliding displacement predictive equations

	Scalar model (eqn 12)	2 parameter vector models (eqn 13)			3parameter vector models (eqn 13)	
	PGA	*GM1=PGA* *GM2=PGV*	*GM1=PGA* *GM2=* T_m	*GM1=PGA* *GM2=* I_a	*GM1=PGA* *GM2=PGV* *GM3=* I_a	*GM1=PGA* *GM2=*T_m *GM3=* I_a
a_1	5.52 (0.09)	-1.56 (0.068)	6.62 (0.059)	2.39 (0.063)	-0.74 (0.063)	4.27 (0.054)
a_2	-4.43 (1.09)	-4.58 (0.63)	-3.93 (0.69)	-5.24 (0.70)	-4.93 (0.57)	-4.62 (0.55)
a_3	-20.39 (4.01)	-20.84 (2.34)	-23.71 (2.56)	-18.78 (2.59)	-19.91 (2.10)	-21.49 (2.04)
a_4	42.61 (5.79)	44.75 (3.38)	49.37 (3.70)	42.01 (3.73)	43.75 (3.03)	46.53 (2.95)
a_5	-28.74 (2.83)	-30.50 (1.65)	-32.94 (1.81)	-29.15 (1.83)	-30.12 (1.48)	-31.66 (1.44)
a_6	0.72 (0.017)	-0.64 (0.013)	0.93 (0.011)	-1.56 (0.019)	-1.30 (0.016)	-0.57 (0.019)
a_7	--	1.55 (0.009)	1.79 (0.012)	1.38 (0.0097)	1.04 (0.012)	1.14 (0.012)
a_8	--	--	--	--	0.67 (0.011)	0.86 (0.0095)
$\sigma_{\ln}$	1.13	Figure 9a / Table 2			Figure9b / Table 2	

The ground motion parameters *PGV*, I_a, T_m, $D_{5\text{-}75}$, and $D_{5\text{-}95}$ were added to the scalar predictive equation with *PGA*. The functional form of these models is:

$$\ln D = a_1 + a_2\left(\frac{k_y}{PGA}\right) + a_3\left(\frac{k_y}{PGA}\right)^2 + a_4\left(\frac{k_y}{PGA}\right)^3 + a_5\left(\frac{k_y}{PGA}\right)^4 + a_6 \ln(PGA) + a_7 \ln(GM2) + a_8 \ln(GM3) + \varepsilon\sigma_{\ln} \quad (13)$$

where *GM2* and *GM3* are the ground motion parameters included in addition to *PGA*. For the models with two ground motion parameters, the *GM3* term is not utilized.

To compare the various models based on the efficiency criterion, the standard deviations of the predicted displacements are plotted versus k_y/PGA in Figure 9. Figure 9a shows the results for vectors of two ground motion parameters, while Figure 9b shows the results for vectors of three ground motion parameters. By adding additional ground motion parameters, the standard deviation decreases significantly, particularly at smaller values of k_y/PGA. The standard deviation is reduced most at small values of k_y/PGA because here the displacement episodes sample more of the ground motion, and thus the information provided by the additional ground

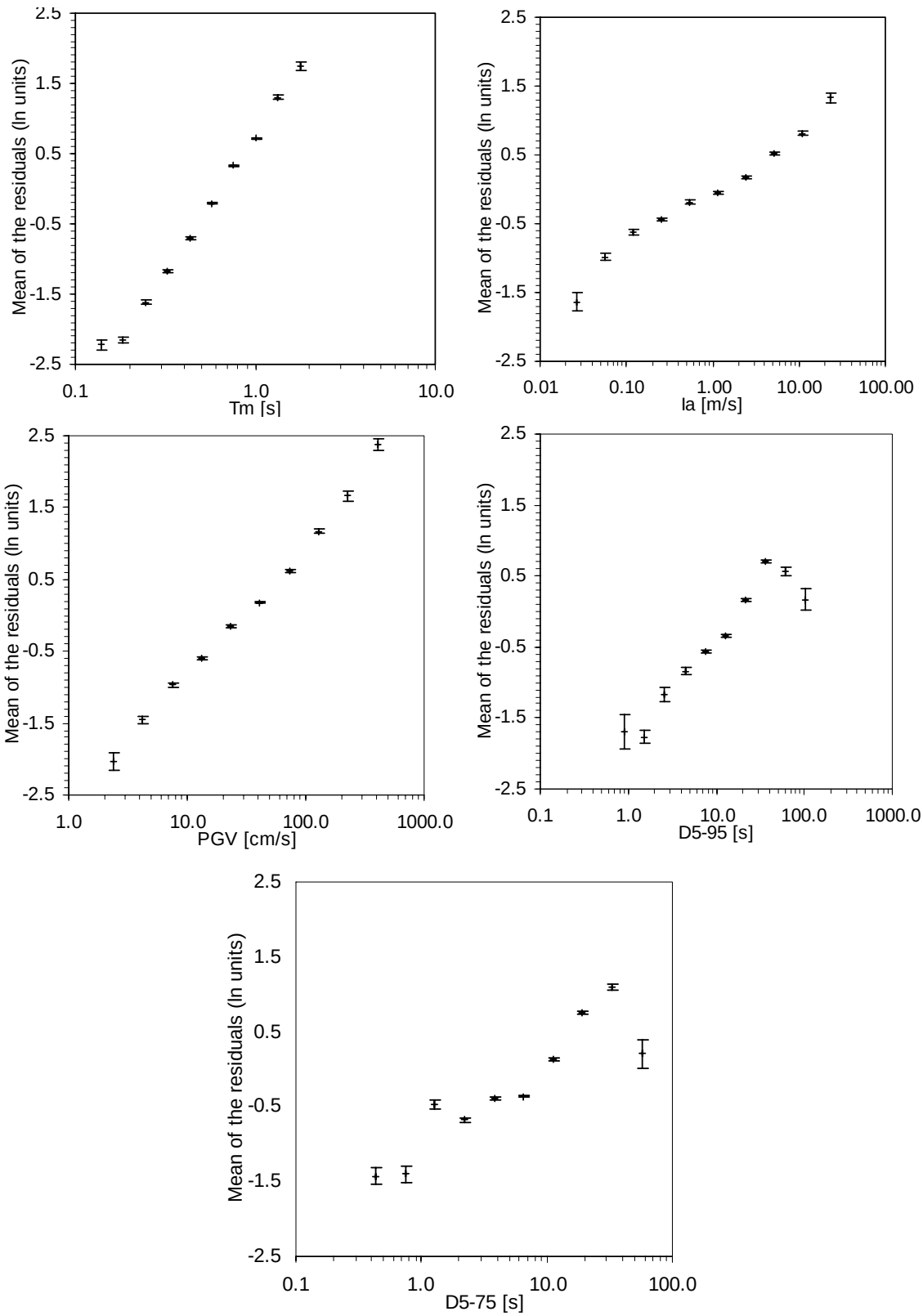

Figure 8: Mean residuals from equation (12) plotted with respect to omitted ground motion parameters

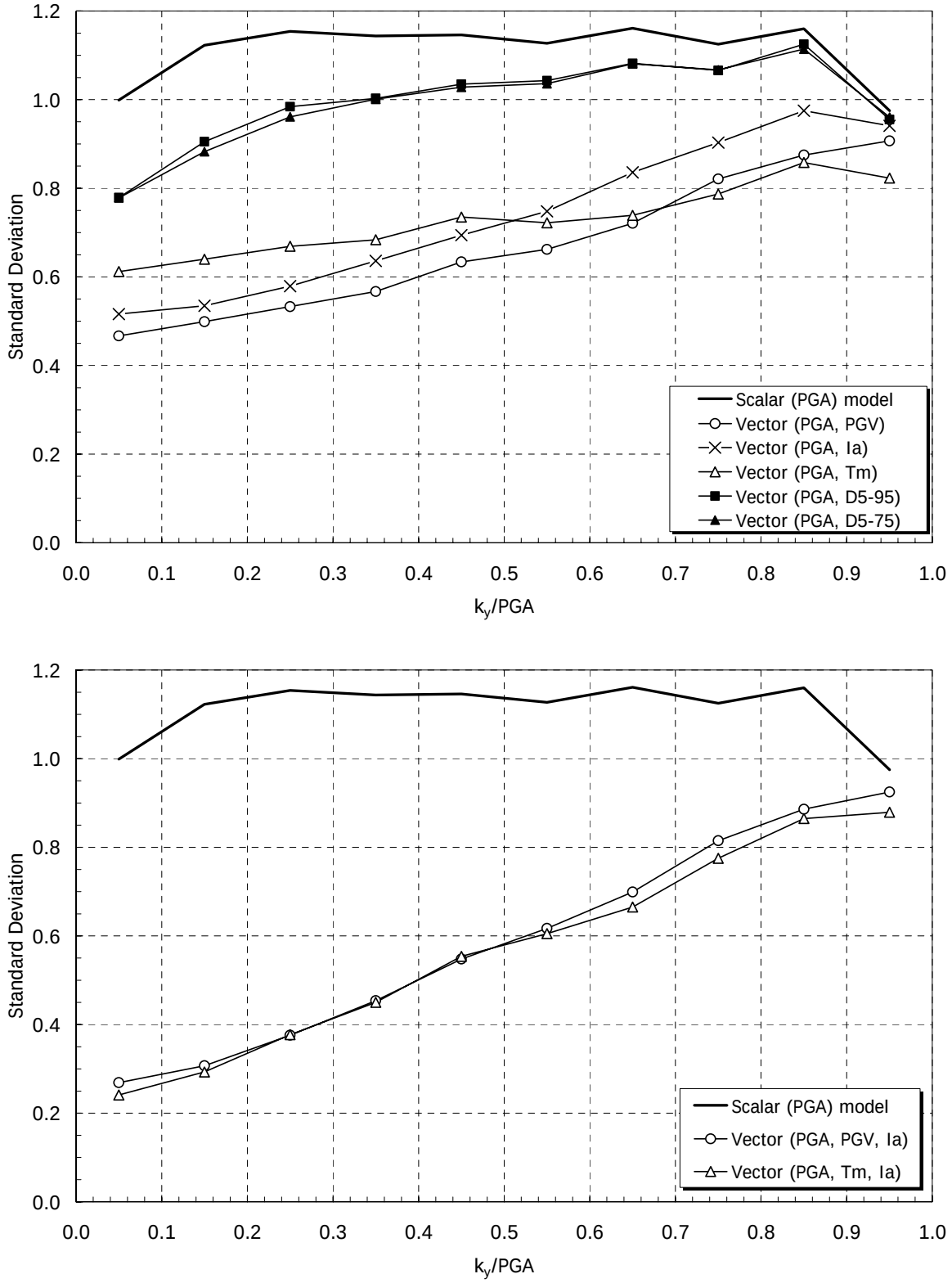

Figure 9: Variation of standard deviation with k_y/PGA for the proposed (a) scalar and two parameter vector models, and (b) the three parameter vector models

motion parameters reduces the standard deviation in the displacement prediction. At large values of k_y/PGA, there are few displacement episodes and each episode is very short, such that little of the ground motion is sampled and adding more ground motion parameters does not reduce the standard deviation. Thus, for all of the models considered, the standard deviation at k_y/PGA > 0.9 was never reduced below about 0.8.

Considering the two ground motion models (Figure 9a), combining *PGA* with the duration parameters ($D_{5\text{-}75}$, $D_{5\text{-}95}$) only reduced the standard deviation 10 to 20%, while combining *PGA* with *PGV*, T_m, or I_a reduced the standard deviation by 40 to 60% at moderate to low values of k_y/PGA. These results are similar to those in Figure 5. For the two ground motion parameter models, the combination of (*PGA*, *PGV*) provides the smallest values of standard deviation. Nonetheless, the (*PGA*, T_m) and (*PGA*, I_a) models are also adequate. The model parameters a_1 through a_7 for the (*PGA*, *PGV*), (*PGA*, T_m), and (*PGA*, I_a) models are provided in Table 1, along with the standard error for each model parameter. The variation of $\sigma_{\ln}$ with k_y/PGA for these three models can be approximated by the linear relationships given in Table 2.

Considering the three ground motion models (Figure 9b), the combinations of (*PGA*, *PGV*, I_a) and (*PGA*, T_m, I_a) produced standard deviations that were 50 to 75% smaller than the scalar (*PGA*) model and 15 to 40% smaller than the two ground motion parameter models. In these cases, I_a is providing additional information regarding the duration of motion, which is not included in either the (*PGA*, *PGV*) or (*PGA*, T_m) models. Using the duration parameters ($D_{5\text{-}75}$, $D_{5\text{-}95}$) in a three ground motion parameter models only reduced the standard deviation by 2 to 5% from the two ground motion parameter models. Thus, for sliding displacement, it appears that I_a is more efficient at providing duration information than either $D_{5\text{-}75}$ or $D_{5\text{-}95}$. The model parameters a_1 through a_8 for the (*PGA*, *PGV*, I_a) and (*PGA*, T_m, I_a) models are given in Table 1, and the linear relationships for $\sigma_{\ln}$ versus k_y/PGA for these models are given in Table 2.

The sufficiency criterion can be addressed by considering the magnitude and distance dependence of the residuals for each predictive model. Figure 10 plots the residuals for the scalar (*PGA*) model, the (*PGA*, *PGV*) two parameter vector model, and the (*PGA*, *PGV*, I_a) three parameter vector model. The mean residuals are shown for overlapping magnitude and distance bins. For the *PGA* model, the mean residuals do not vary with distance, but they significantly increase with increasing magnitude. This trend indicates that *PGA* alone does not sufficiently predict sliding displacement because it does not fully describe the ground motion and its variation with magnitude. However, the addition of the second and third ground motion parameters to the displacement predictive model results in residuals that do not vary significantly with magnitude or distance. Thus, the vector models satisfy the sufficiency criterion for probabilistic seismic hazard analysis.

Table 2: Standard deviations for the proposed sliding displacement predictive equations

Model	Standard Deviation
2GM (PGA, PGV)	$\sigma_{\ln} = 0.41 + 0.52 \cdot \left(\frac{k_y}{PGA} \right)$
2GM (PGA, T_m)	$\sigma_{\ln} = 0.60 + 0.26 \cdot \left(\frac{k_y}{PGA} \right)$
2GM (PGA, I_a)	$\sigma_{\ln} = 0.46 + 0.56 \cdot \left(\frac{k_y}{PGA} \right)$
3GM (PGA, PGV, I_a)	$\sigma_{\ln} = 0.20 + 0.79 \cdot \left(\frac{k_y}{PGA} \right)$
3GM (PGA, T_m, I_a)	$\sigma_{\ln} = 0.19 + 0.75 \cdot \left(\frac{k_y}{PGA} \right)$

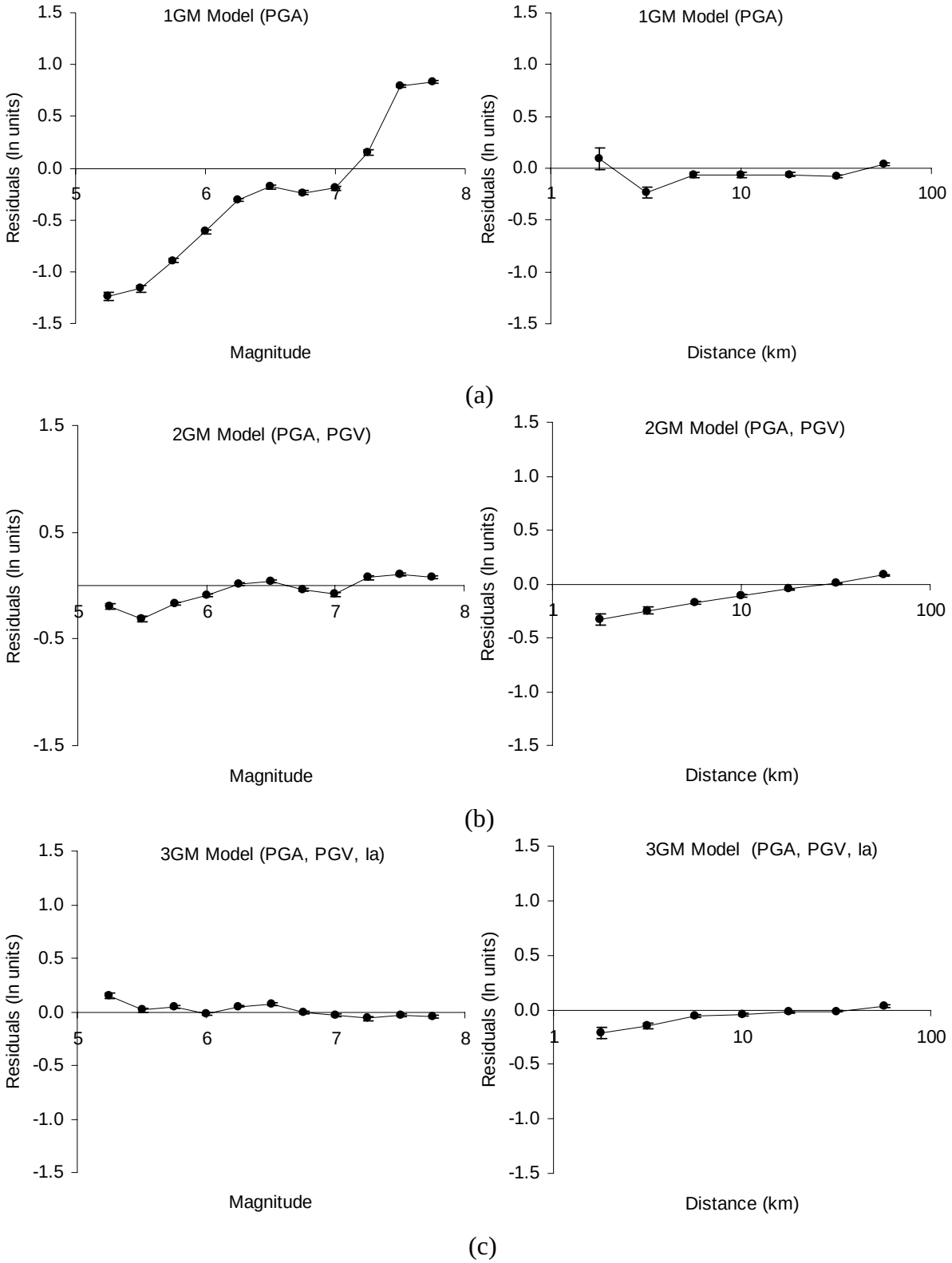

Figure 10: Mean residuals with respect to magnitude and distance for (a) scalar (PGA) model, (b) two parameter (PGA, PGV) vector model, and (c) three parameter (PGA, PGV, I_a) vector model

GROUND MOTION CORRELATION

To implement the vector hazard approach, the correlation coefficient (ρ) between the ground motion parameters used in the sliding displacement model (*GM1, GM2*) is required (equations 8 and 9). The correlation coefficient takes on values between -1.0 and +1.0; positive values indicate that the values of *GM1* and *GM2* for a ground motion both tend to be large (or small), while negative values indicate that when one *GM* is large then the other *GM* tends to be small (or vice versa). A correlation coefficient of 0.0 indicates that the two parameters are not correlated.

The correlation coefficient was computed for the pairs of ground motion parameters identified for the predictive equations of sliding displacement. Using the methodology outlined by Baker and Cornell (2006a), the correlation coefficients were computed using the normalized residuals (ε_{GM}) for each ground motion parameter with respect to a ground motion prediction equation using:

$$\varepsilon_{GM} = \frac{\ln GM_{observed} - \ln GM_{predicted}}{\sigma_{GM}} \tag{14}$$

where $\ln GM_{observed}$ is the natural log of the observed ground motion, $\ln GM_{predicted}$ is the natural log of the predicted ground motion from the ground motion prediction equation, and σ_{GM} is the standard deviation from the ground motion prediction equation. The use of the normalized residuals removes the effects of magnitude, distance, site conditions, etc., as well as any heteroscedasticity, from the variations in the observed ground motion parameters.

The linear relation between ε_{GM} and the ground motion value implies that the correlation coefficient calculated using ε_{GM} also applies to the ground motion parameters themselves (Baker and Cornell 2006a). Therefore, the correlation coefficients between the ground motion parameters can be computed using the values of ε_{GM} and the point estimate for the sample correlation coefficient (Devore 2000):

$$\rho_{GM1,GM2} = \frac{\sum_{i=1}^{n}(\varepsilon_{GM1i} - \overline{\varepsilon_{GM1}})(\varepsilon_{GM2i} - \overline{\varepsilon_{GM2}})}{\sqrt{\sum_{i=1}^{n}(\varepsilon_{GM1i} - \overline{\varepsilon_{GM1}})^2 \sum_{i=1}^{n}(\varepsilon_{GM2i} - \overline{\varepsilon_{GM2}})^2}} \tag{15}$$

where $\rho_{GM1,GM2}$ is the correlation coefficient between GM1 and GM2, ε_{GM1i} and ε_{GM2i} are the ith observations of ε_{GM1} and ε_{GM2}, $\overline{\varepsilon_{GM1}}$ and $\overline{\varepsilon_{GM2}}$ are the sample means of ε_{GM1} and ε_{GM2}, and *n* is the total number of observations.

The developed models use the ground motion parameters *PGA*, peak ground velocity (*PGV*), Arias Intensity (I_a), and mean period (T_m). The correlation coefficients between each pair of these parameters were computed using currently available ground motion prediction equations (Table 3). To investigate the impact of different ground motion prediction models, three different models for PGA were coupled with the other models.

Table 3. Ground motion prediction equations used in correlation analysis

GM	Model	No. Motions
PGA	BA: Boore and Atkinson (2006)	901
PGA	CB: Campbell and Bozorgnia (2006)	901
PGA	CY: Chiou and Youngs (2006)	901
PGV	BA: Boore and Atkinson (2006)	901
I_a	T: Travasarou et. al. (2003)	765
T_m	R: Rathje et. al. (2004)	544

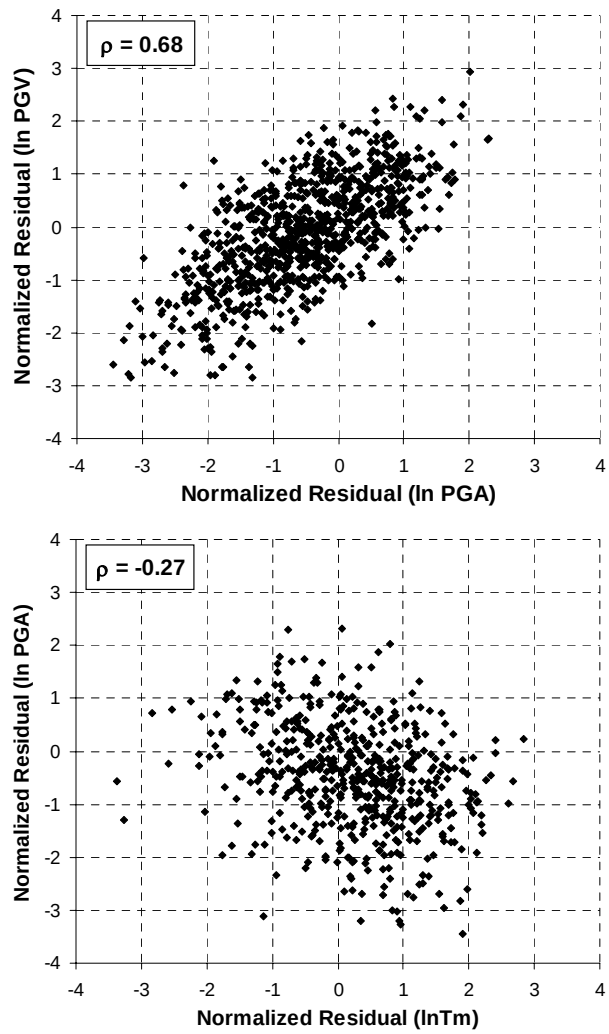

Figure 11. Scatter plot of normalized residuals for (a) PGA, PGV and (b) PGA, T_m used to compute correlation coefficient

To compute the normalized residuals, $\ln GM_{predicted}$ and σ_{GM} were calculated for each motion using the ground motion prediction equation and the magnitude, distance, and additional

parameters (e.g., site class, fault type), while $\ln GM_{observed}$ was calculated directly from the recording. The two horizontal components of each ground motion were combined using the methodology outlined in each ground motion prediction equation before being used in equation (14).

The initial number of unscaled motions used to develop the displacement models was over 2,000, which includes separate horizontal components. Combining the two horizontal components and removing single components reduced the total number of data to 1,011 motions. Further reductions in the data were caused by removing motions where all parameters in the ground motion prediction equation were not available (e.g., Joyner-Boore distance missing) or beyond the limitations of the prediction equation (e.g., distance greater than 100 km). The resulting datasets include 901 motions for *PGA* and *PGV*, 765 motions for I_a, and 545 motions for T_m. Examples of the data used to compute the correlation coefficients for *PGA*, *PGV* and *PGA*, T_m are shown in Figure 11. The *PGA*, *PGV* data in Figure 11 fall in a relatively small band and the computed value of $\rho_{PGA,PGV}$ is 0.68. The *PGA*, T_m data show significantly more scatter and the data have a slight negative slope. The resulting value of $\rho_{PGA,Tm}$ is -0.27.

The calculated values of correlation coefficient are summarized in Table 4. *PGA* and I_a display the highest correlation ($\rho_{PGA,Ia}$ = 0.83), which is not surprising because I_a is derived from the integral of the square of the acceleration-time history. A similar value was reported by Baker (2007). *PGA* and *PGV* are also highly correlated ($\rho_{PGA,PGV}$ ~ 0.6), as are I_a and *PGV* ($\rho_{Ia,PGV}$ = 0.64). The range of values computed for $\rho_{PGA,PGV}$ when using different combinations of ground motion prediction equations was somewhat large ($\rho_{PGA,PGV}$ =0.54 to 0.68), but demonstrates the uncertainty in the computed values.

The other combinations of ground motion parameters exhibit less correlation. T_m displays negative and low levels of correlation with both *PGA* and I_a ($\rho_{PGA,Tm}$ = -0.27, $\rho_{Ia,Tm}$ = -0.19), which is clearly indicated in the scatter plot in Figure 11. The negative values of correlation for $\rho_{PGA,Tm}$ and $\rho_{Ia,Tm}$ are due to the fact that high intensity records, particularly those with large *PGA*, are generally associated with more high frequency content and thus smaller values of T_m. The smaller values of correlation are a result of T_m being a parameter that is not affected by intensity, while *PGA* and I_a are significantly affected by intensity. Finally, *PGV* and T_m display some positive correlation ($\rho_{PGV,Tm}$ = 0.24), which is due to the fact that *PGV* is affected by the motion at moderate periods and T_m provides information about frequency content.

The correlation coefficients reported here should be considered preliminary estimates of the true ground motion correlation. Various issues related to inter-event and intra-event correlation have not been addressed as they are beyond the scope of this paper, but will be considered in future work. Nonetheless, the correlation coefficients presented here allow for an initial application of the vector hazard approach to predict displacement hazard curves.

Table 4. Correlation coefficient values for various ground motion parameters

GM Pair	$\rho_{GM1,GM2}$	Predictive Models Used
PGA, I_a	0.83	BA, T
PGA, *PGV*	0.68 0.58 0.60 0.54 0.62 0.61	BA, BA CB, CB BA, CB CB, BA CY, BA CY, CB
PGA, T_m	-0.27	BA, R
PGV, I_a	0.64	BA, T
PGV, T_m	0.24	BA, R
I_a, T_m	-0.19	T, R

DEVELOPMENT OF DISPLACEMENT HAZARD CURVES

To demonstrate the development of scalar and vector displacement hazard curves, a hypothetical example is developed. A shallow, infinite slope with k_y = 0.1 is considered and the sliding displacement predictive equations presented in this study are used. Specifically, the *PGA* model and the *PGA*, *PGV* model are used. The seismological model is very simple and based on an exercise in Kramer (1996). A point source is considered at a distance of 5 km with discrete magnitude probabilities of 0.675, 0.225, 0.075, and 0.025 for magnitudes of 4, 5, 6, and 7, respectively. The activity rate (λ_o) is 0.2.

Ground Motion Hazard

Using the ground motion prediction equations of Boore and Atkinson (2006) for rock conditions (V_s = 760 m/s), the resulting scalar hazard curves (*MRE*) for *PGA* and *PGV* are shown in Figures 12a and b, respectively. The *MRE* hazard curves traditionally are used to develop design ground motion levels for a selected return period, typically either 475 years (λ = 0.0021 1/yr, 10% probability of exceedance in 50 years) or 2,475 years (λ = 0.0004 1/yr, 2% probability of exceedance in 50 years). For the curves shown, the ground motion levels with a 475 year return period are *PGA*=0.5 g and *PGV*=38 cm/s, while the 2,475 year ground motion levels are *PGA*=0.8 g and *PGV*=68 cm/s. The derivatives of the *PGA* and *PGV* scalar hazard curves, which represent the scalar mean rate densities (*MRD*) for the two parameters, also are shown in Figure 12. These *MRD* curves, which are analogous to probability density functions, demonstrate the likelihood of different values of *PGA* and *PGV*.

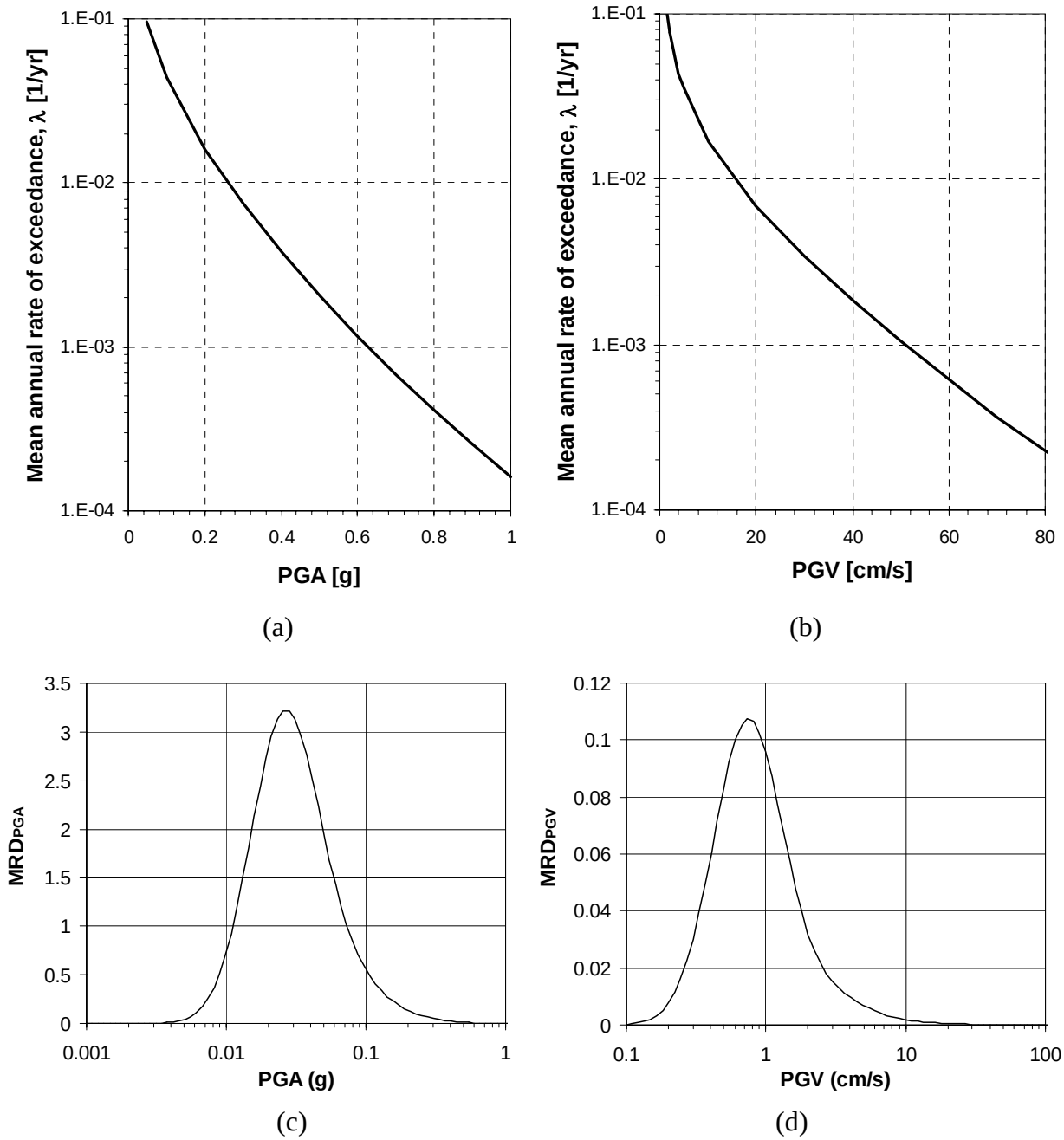

Figure 12. Scalar representation of MRE hazard for (a) PGA and (b) PGV; MRD hazard for (c) PGA and (d) PGV

For the scalar approach using only *PGA* to predict sliding displacement, the *PGA MRD* curve (Figure 12c), which represents the probability of occurrence of each value of *PGA*, is used with equation (4) to compute the hazard for a range of displacement levels. For the vector approach, the scalar *PGA* and *PGV MRD* curves are not used, but rather the *MRD* of the joint occurrence of *PGA*, *PGV* pairs are computed using equation (6). Figure 13 shows the joint *MRD* for *PGA*, *PGV* for this example using $\rho_{PGA,PGV}$ = 0.0 and 0.6. The *MRD* is shown as contours because it is

a 3D surface with *PGA* and *PGV* on the *x* and *y* axes, and the rate occurrence on the *z* axis. When ρ = 0.0 (Figure 13a), the occurrence of *PGA* and *PGV* are assumed independent and the *MRD* contours are circular for each event. When each event is combined and weighted by its probability of occurrence, the final *MRD* displays a 'tail' at the larger values of *PGA* and *PGV* because of the lower probability of the large events. When ρ = 0.6 (Figure 13b), the *MRD* contours are oval-shaped for each event, resulting in an oval shape for the full *MRD*, although a 'tail' is still observed at large *PGA*, *PGV* pairs. Comparing the *MRD* contours in Figure 13, ρ > 0.0 produces larger rates of joint occurrence of large values of *PGA* and *PGV*, but smaller rates of joint occurrence of large values of *PGA* coupled with small values of *PGV* (and vice versa). Thus, the positive correlation denotes that it is more likely that large (or small) values of *PGA* and *PGV* jointly occur at the same location during the same earthquake.

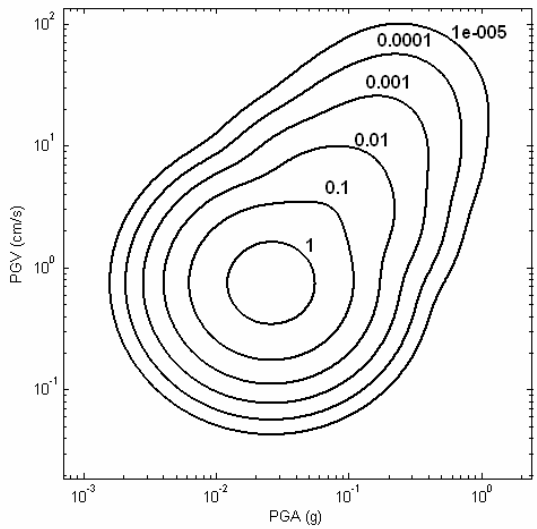

(a)

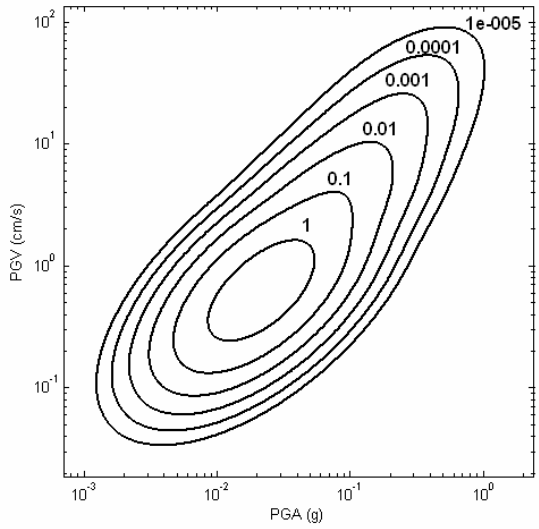

(b)

Figure 13. Vector representation of MRD PGA, PGV hazard for (a) ρ = 0.0 and (b) ρ = 0.6

Displacement Hazard Curves

The displacement hazard curves derived from the scalar *MRD* for *PGA* (Figure 12) and the vector *MRD* for *PGA*, *PGV* (Figure 13) are shown in Figure 14. It is clear from Figure 14 that the vector approach reduces the displacement hazard substantially. The hazard is reduced when using multiple ground motion parameters due to changes in both the median displacement prediction and the standard deviation of the prediction. For the developed displacement models, the median displacement is smaller when using the *PGA*, *PGV* predictive equation and the standard deviation is also smaller (Figure 9). Both of these characteristics result in a smaller hazard.

The hazard curves in Figure 14 are used to assess the displacement levels for different levels of hazard. The displacement with a 10% probability of exceedance in 50 years is about 55 cm when using the scalar *PGA* model, but it is reduced to 17 cm when using the vector *PGA*, *PGV* model. The displacement with a 2% probability of exceedance in 50 years is greater than 200 cm when using the scalar model, but only 65 cm when using the vector model. For this example, the use of the vector model reduces the displacement hazard by more than 50%.

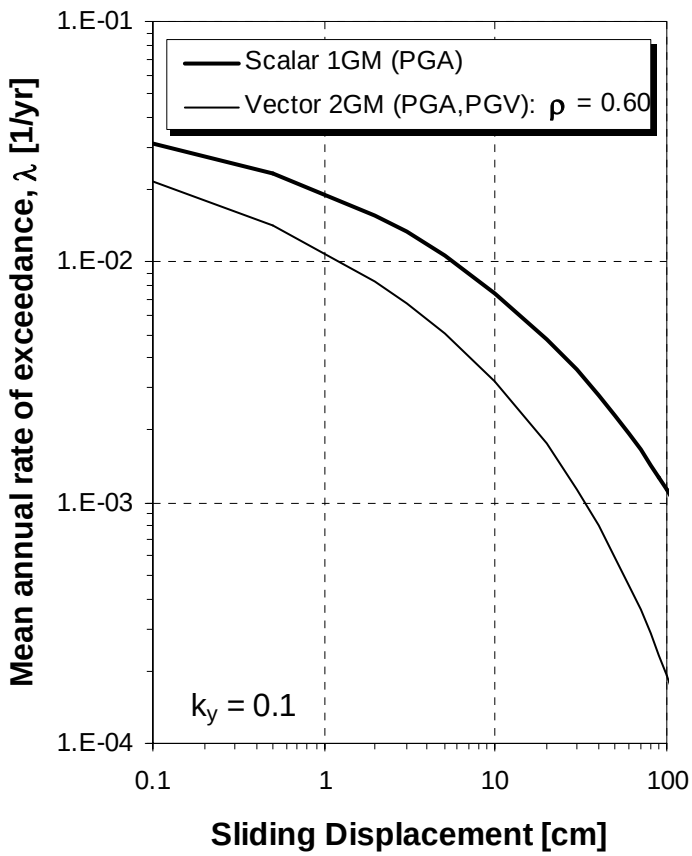

Figure 14. Displacement hazard curves from scalar and vector approaches

Some engineers use a ground motion for a specific hazard level in an analysis and assume that the response of the system to this motion has the same level of hazard as the ground motion (Figure 2, Probabilistic Ground Motion approach). However, this is not the case because it ignores the uncertainty in the displacement prediction. For example, if the 10% in 50 year *PGA*

of 0.5 g (Figure 12) is used in the scalar displacement model, the predicted median displacement is 37 cm, as opposed to the 10% in 50 year displacement of 55 cm from the scalar model in Figure 14. Using the 2% in 50 year *PGA* of 0.8 g, the scalar model predicts a median displacement of only 96 cm, as opposed to the 2% in 50 year displacement of 233 cm. The fully probabilistic values from Figure 14 are larger in this case because they consider the significant aleatory variability in the displacement prediction. When considering the vector (*PGA*, *PGV*) model, the 10% in 50 year ground motion levels predict a median displacement of 22 cm while the vector hazard curve in Figure 14 indicates a value of 17 cm. At 2% in 50 years, the ground motions predict a median displacement of 74 cm while the vector hazard curve predicts 65 cm. In this case, the fully probabilistic displacements using the vector model are smaller than the median displacements predicted from the probabilistic ground motions. This result, which is the opposite from what was observed for the scalar case, is caused by the smaller $\sigma_{\ln}$ for the vector model and the fact that the correlation between *PGA* and *PGV* was taken into account when performing the fully probabilistic analysis and ignored when using the probabilistic ground motions. These comparisons demonstrate that using a ground motion for a given hazard level in a sliding displacement calculation does not produce a displacement with the same hazard level. As the goal in performance-based engineering is to predict the performance of a slope for given hazard level, the displacement hazard curve is suited for this purpose.

The correlation coefficient between the ground motion parameters used in the vector analysis plays a significant role in the hazard calculation (equations 8 and 9). Figure 15 displays displacement hazard curves from the *PGA*, *PGV* vector model using values of ρ equal to -0.8, 0.0, and + 0.8. A positive value of ρ increases the hazard, while a negative value decreases the hazard as compared with the curve for $\rho = 0.0$. Because positive correlation indicates that large values of *GM1* are coupled with large values of *GM2* and because displacement increases with increasing values of *GM1* and *GM2*, positive values of ρ result in larger computed values of displacement. Negative correlation indicates that large values of *GM1* are coupled with small values of *GM2*, and thus smaller displacements are calculated and the hazard is reduced.

In the previous sections, three different two-parameter vector models were developed for sliding displacement. Although the *PGA*, *PGV* model is recommended for use because its standard deviation is the smallest, the other models (*PGA*, I_a and *PGA*, T_m) display only slightly larger values of standard deviation. Figure 16 presents displacement hazard curves all three of these three two parameter vector models. When using the appropriate correlation coefficient between the pairs of ground motion parameters ($\rho_{PGA,PGV} = 0.6$, $\rho_{PGA,Ia} = 0.83$, $\rho_{PGA,Tm} = -0.27$; Table 2), the three models produce remarkably similar displacement hazard curves (Figure 16a). This result appears quite fortuitous and it is not clear whether similar results would be found for vector hazard analyses for other applications. The displacement hazard curves for the three vector models are shown for $\rho = 0.0$ in Figure 16b. Here a clear difference is observed, with *PGA*, *PGV* and *PGA*, I_a displaying similar curves and *PGA*, T_m displaying a larger hazard. These differences are due to the fact that the *PGA*, T_m model predicts very large displacements when large values of *PGA* and T_m jointly occur. However, large values of *PGA* and T_m are not likely to occur because of the negative correlation between these ground motion parameters (Table 4). Thus, the resulting displacement hazard curves are only meaningful when the appropriate correlation between the input ground motion parameters is modeled.

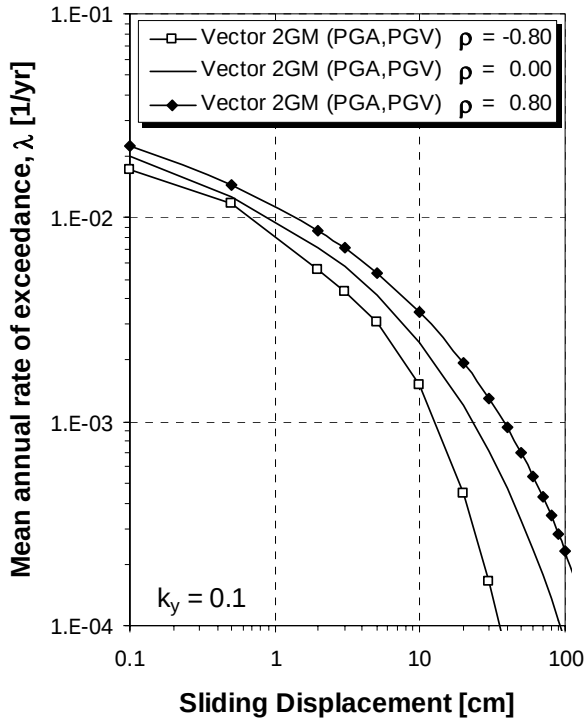

Figure 15. Effect of ρ on displacement hazard curve

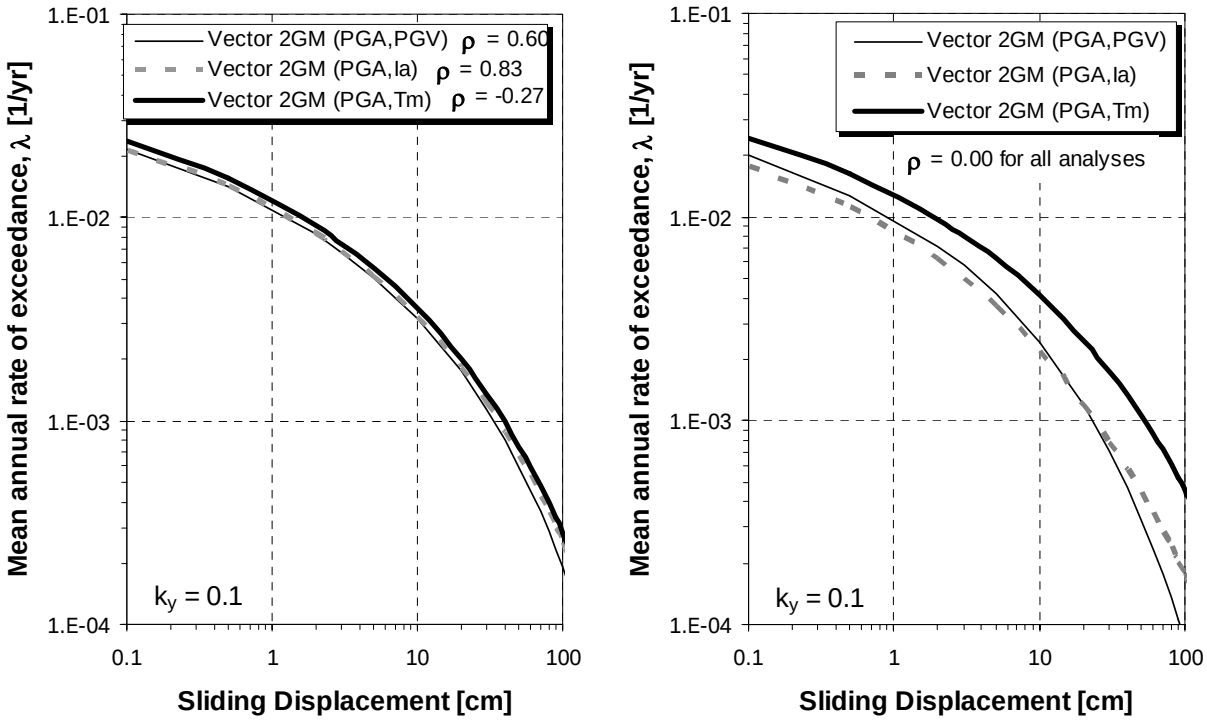

(a) (b)

Figure 16. Displacement hazard curves developed from different vector models
(a) $\rho \neq 0$ and (b) $\rho=0$

CONCLUSIONS

A fully probabilistic assessment of sliding displacement of slopes is a valuable tool because it rigorously accounts for the variability in the ground motion and the variability in the sliding displacement prediction. Both of these sources of variability, as quantified by $\sigma_{\ln}$, are significant and ignoring them may result in non-conservative estimates of sliding displacement. The fully probabilistic approach produces a displacement hazard curve, and can be formulated in terms of a scalar or vector of ground motion parameters. The vector framework is based on the work of Bazzurro and Cornell (2002) who applied it to the hazard assessment of inter-story drift of a 20-story building. Beyond the requirements of a scalar probabilistic seismic hazard analysis, the only additional information required for a vector analysis is the correlation coefficient between the ground motion parameters used in the model of sliding displacement.

This report describes the development of empirical predictive models for rigid block sliding displacement that are a function of multiple ground motion parameters. Multiple ground motion parameters are used in an effort to reduce the standard deviation of the displacement prediction. Compared with the scalar model using only one ground motion parameter (*PGA*), vector models using two ground motion parameters result in a 40 to 60% reduction in the standard deviation. The vector (*PGA*, *PGV*) produces the smallest standard deviation, while the vectors (*PGA*, T_m) and (*PGA*, I_a) produce slightly larger values. The duration parameters $D_{5\text{-}75}$ and $D_{5\text{-}95}$ do not significantly reduce $\sigma_{\ln}$. For each of these vectors, the reduction in $\sigma_{\ln}$ is most significant at smaller values of k_y/PGA because at smaller values of k_y/PGA more of the ground motion is sampled during the displacement calculation and thus the information provided by the additional ground motion parameters improves the displacement prediction. The three parameter vector models (*PGA*, *PGV*, I_a and *PGA*, T_m, I_a) further reduce $\sigma_{\ln}$ by 15 to 40% at smaller values of k_y/PGA. Based on their ability to significant reduce $\sigma_{\ln}$ for the displacement prediction, the two parameter vector model of (*PGA*, *PGV*) and the three parameter vector model of (*PGA*, *PGV*, I_a) are recommended for use.

A hypothetical example was used to demonstrate the vector framework for sliding displacement. Displacement hazard curves were developed for a yield acceleration of 0.1 g using scalar and vector models. For this example, the displacement hazard was reduced by as much as 50% when using the vector approach as opposed to the scalar approach. This reduction in hazard is due to the reduction in the standard deviation of the displacement prediction when using a vector model, as well as the change in the median displacement prediction. The displacement hazard curve was used to identify displacement levels for different hazard levels (10% in 50 years and 2% in 50 years), and it was shown that using ground motions for a given hazard level does not produce a displacement level with the same level of hazard.

The fully probabilistic assessment of the sliding displacement of slopes represents a step forward because it accounts for the main sources of variability in the problem and it quantifies the probability of exceedance for different displacement levels. In the future, the framework described here may be used on a regional scale to assess earthquake-induced landslide hazards or on a local scale to assess the performance of engineered slopes and earth structures.

REFERENCES

Ambraseys, N.N., Menu, J.M., 1988. "Earthquake-induced ground displacements" *Earthquake Engineering and Structural Dynamics* 16, 985–1006

Ambraseys, N.N. and Srbulov, M. 1994. "Attenuation of Earthquake-Induced Displacements," *J. Earthquake Engineering and Structural Dynamics*, V. 23, pp. 467-487.

Baker, J.W. 2007. "Correlation of ground motion intensity parameters used for predicting structural and geotechnical response," *10th International Conference on Applications of Statistics and Probability in Civil Engineering*, Tokyo, Japan.

Baker, J.W. and Cornell, C.A. 2005. "A Vector-Valued Ground Motion Intensity Measure Consisting of Spectral Acceleration and Epsilon." *Earthquake Engineering & Structural Dynamics*, 34 (10), 1193-1217.

Bazzurro, P. and Cornell, C. A. 2002. Vector-valued probabilistic seismic hazard analysis, in Proceedings, 7th U.S. National Conference on Earthquake Engineering, Boston, Mass. 10 pp.

Benjamin, J.R. and Cornell, C.A. 1970. *Probability, Statistics, and Decision for Civil Engineers*, McGraw Hill Co., New York, NY.

Boore, D. M. and Atkinson, G. M. 2006. Boore-Atkinson NGA empirical ground-motion model for the average horizontal component of PGA, PGV and SA at spectral periods of 0.1, 0.2, 1, 2 and 3 seconds: Interim report for USGS review (to be finalized for the PEER-NGA project)

Boore, D. M., Joyner, W. B., and Fumal, T. E., 1997. Equations for estimating horizontal response spectra and peak acceleration from western North American earthquakes: A summary of recent work, *Seismological Research Letters* **68** (1), 128–153.

Bray, J.D. and Rathje, E.M. 1998. "Earthquake-Induced Displacements of Solid-Waste Landfills," *J. of Geotechnical and Geoenvironmental Engineering*, ASCE, 124(3), 242-253.

Bray, J.D. Travasarou, T. 2007. "Simplified Procedure for Estimating Earthquake-Induced Deviatoric Slope Displacements", *J. Geotech. and Geoenvir. Engrg.*, 133(4), 381-392

Bray, J.D., Rathje, E.M., Augello, A.J., and Merry, S.M. 1998 "Simplified Seismic Design Procedure for Lined Solid-Waste Landfills," *Geosynthetics International*, **5**(1-2): 203-235.

Cornell, C. A., and Luco, N., 2001. "Ground motion intensity measures for structural performance assessment at near-fault sites," Proceedings of the *U.S.-Japan joint workshop and third grantees meeting, U.S.-Japan Coop. Res. on Urban EQ. Disaster Mitigation*, Seattle, Washington.

Del Gaudio, V., Pierri, P., and Wasowski, J. 2003. "An Approach to Time-Probabilistic Evaluation of Seismically Induced Landslide Hazard," *Bulletin of the Seismological Society of America*, 93(2), 557-569.

Devore, J.L. 2000. *Probability and Statistics for Engineering and the Sciences, 5th Ed*. Duxbury, California.

Franklin, A.G., Chang, F.K., 1977. "Earthquake resistance of earth and rock-fill dams" US Army Corps of Engineers Waterways Experiment Station Miscellaneous Paper vol. S-71-17. 59 pp.

Jibson, R.W. and Jibson, M. 2003. "Java Programs for using Newmark's method and simplified decoupled analysis to model slope performance during earthquakes," U.S. Geological Survey Open-File Report, 03-005. U.S. Geological Survey, Denver, CO.

Jibson, R.W. and Jibson, M. 2006. Personal Communication.

Jibson, R.W. Harp, E.L. and Michael, J.A. 2000. "A method for producing digital probabilistic seismic landslide hazard maps", *Engineering Geology*, 58, 271-289.

Kramer,S.L. 1996. *Geotechnical Earthquake Engineering*, Prentice-Hall, Upper Saddle River, NJ.

Makdisi, F. I., and Seed, H. B. 1978. "Simplified Procedure for Estimating Dam and Embankment Earthquake Induced Deformations," *Journal of the Geotechnical Engineering Division*, ASCE, Vol 104, No. GT7, pp 849-867.

Newmark, N.M. 1965. "Effects of earthquakes on dams and embankments," *Geotechnique*, 15(2), p. 139-160.

Rathje, E.M. and Bray, J.D. 1999. "An Examination of Simplified Earthquake-Induced Displacement Procedures for Earth Structures," *Canadian Geotechnical J.*, 36(1), 72-87.

Rathje, E.M. and Bray, J.D. 2000. "Nonlinear Coupled Seismic Sliding Analysis of Earth Structures," *Journal of Geotechnical and Geoenvironmental Engineering*, ASCE, 126(11), pp. 1002-1014.

Rathje, E.M., Faraj, F., Russell, S., and Bray, J.D. 2004. "Empirical Relationships for Frequency Content Parameters of Earthquake Ground Motions," *Earthquake Spectra*, Earthquake Engineering Research Institute, 20(1), 119-144.

Rathje, E.M. and Saygili,G. 2008. "Probabilistic Seismic Hazard Analysis for the Sliding Displacement of Slopes: Scalar and Vector Approaches," submitted to *Journal of Geotechnical and Geoenvironmental Engineering*, ASCE.

Saygili, G. and Rathje, E.M. 2008. "Empirical Predictive Models for earthquake-Induced Sliding Displacements of Slopes," submitted to the *Journal of Geotechnical and Geoenvironmental Engineering*, ASCE.

Seed, H.B. and G.R. Martin. 1966. "The seismic coefficient in earth dam design" A*SCE J. of Soil Mech. Found. Div*. 92(SM3) 25-58.

Travasarou, T., Bray, J.D. and Abrahamson, N.A. 2003. "Empirical attenuation relationship for Arias intensity" *Earthquake Engineering and Structural Dynamics* 32: 1133–1155

Travasarou, T., Bray, J.B., and Der Kiureghian, A. 2004. "A Probabilistic Methodology for Assessing Seismic Slope Displacements," Proceedings, *13th World Conference on Earthquake Engineering*, Paper 2326, Vancouver, Canada, August.

Travasarou T. 2003. "Optimal ground motion intensity measures for probabilistic assessment of seismic slope displacements" Ph.D. Dissertation, Department of Civil and Environmental Engineering, University of California, Berkeley, CA.

Watson-Lamprey, J. Abrahamson, N 2006. "Selection of ground motion time series and limits on scaling", *Soil Dynamics and Earthquake Engineering*, Vol. 26, no. 5, pp. 477-482.

Yegian, M.K., Marciano, E.A., Ghahraman, V.G., 1991a. "Seismic Risk Analysis for Earth Dams" *Journal of Geotechnical Engineering* 117, 18-34.

Yegian, M.K., Marciano, E.A., Ghahraman, V.G., 1991b. "Earthquake-induced permanent deformations: probabilistic approach" *Journal of Geotechnical Engineering* 117, 35–50.

PUBLICATIONS RESULTING FROM THIS WORK

Rathje, E.M. and Saygili, G. 2006. "A Vector Hazard Approach for Newmark Sliding Block Analyses," *Earthquake Geotechnical Engineering Workshop*, University of Canterbury, Christchurch, New Zealand, 20-23 November.

Rathje, E.M. and Saygili,G. 2008. "Probabilistic Seismic Hazard Analysis for the Sliding Displacement of Slopes: Scalar and Vector Approaches," submitted to the *Journal of Geotechnical and Geoenvironmental Engineering*, ASCE.

Saygili, G. and Rathje, E.M. 2008. "Empirical Predictive Models for earthquake-Induced Sliding Displacements of Slopes," submitted to the *Journal of Geotechnical and Geoenvironmental Engineering*, ASCE.